European Journal of Medicinal Chemistry 131 (2017) 1–13

Contents lists available at ScienceDirect

European Journal of Medicinal Chemistry

journal homepage: http://www.elsevier.com/locate/ejmech

Research paper

Development of 2, 4-diaminoquinazoline derivatives as potent PAK4 inhibitors by the core refinement strategy

Chenzhou Hao [a, 1], Wanxu Huang [a, d, 1], Xiaodong Li [b, c], Jing Guo [a], Meng Chen [b, c], Zizheng Yan [a], Kai Wang [a], Xiaolin Jiang [a], Shuai Song [a], Jian Wang [a], Dongmei Zhao [a, *], Feng Li [b, c, **], Maosheng Cheng [a, ***]

[a] Key Laboratory of Structure-Based Drug Design & Discovery of Ministry of Education, Shenyang Pharmaceutical University, Shenyang 110016, China
[b] Department of Cell Biology, Key Laboratory of Cell Biology, Ministry of Public Health, China Medical University, Shenyang 110001, China
[c] Key Laboratory of Medical Cell Biology, Ministry of Education, China Medical University, Shenyang 110001, China
[d] School of Life Science and Bio-pharmaceutics, Shenyang Pharmaceutical University, Shenyang 110016, China

ARTICLE INFO

Article history:
Received 4 January 2017
Received in revised form
24 February 2017
Accepted 27 February 2017

Keywords:
p21-activated kinase
PAK4 inhibitor
Synthesis
Anti-cancer
2,4-diaminoquinazoline

ABSTRACT

Upon analysis of the reported crystal structure of PAK4 inhibitor KY04031 (PAK4 IC_{50} = 0.790 μM) in the active site of PAK4, we investigated the possibility of changing the triazine core of KY04031 to a quinazoline. Using KY04031 as a starting compound, a library of 2, 4-diaminoquinazoline derivatives were designed and synthesized. These compounds were evaluated for PAK4 inhibition, leading to the identification of compound **9d** (PAK4 IC_{50} = 0.033 μM). Compound **9d** significantly induced the cell cycle in the G1/S phase and inhibited migration and invasion of A549 cells that over-express PAK4 via regulation of the PAK4-LIMK1 signalling pathway. A docking study of compound **9d** was performed to elucidate its possible binding modes and to provide a structural basis for further structure-guided design of PAK4 inhibitors. Compound **9d** may serve as a lead compound for anticancer drug discovery and as a valuable research probe for further biological investigation of PAK4.

1. Introduction

p21-activated kinases (PAKs) are serine/threonine (Ser/Thr) protein kinases that are downstream signalling effectors of the Rho/Rac family of GTPases [1]. The six known mammalian PAK isoforms are grouped into two subgroups, PAK1-3 (group I) and PAK4-6 (group II), based on their structural and functional characteristics [2]. PAKs have been shown to be important for regulation of the actin cytoskeleton, focal adhesion contacts and cell motility and are positioned at the nexus of several oncogenic signalling pathways.

Among the group II PAKs, PAK4 is overexpressed at a high frequency in several malignancies including those of the colon, breast, pancreas, thyroid, and ovaries [3–5]. It has been linked to many hallmarks of tumorigenesis, including anchorage-independent growth [3], angiogenesis [6], increased cell survival [7], migration [8], and invasion [8,9]. Therefore, PAK4 is a promising target for the development of cancer therapeutics [1,10].

A number of groups have previously reported inhibitors of PAK4 as cancer treatments (Fig. 1) [11,12]. Among this studies, only one pan-PAK inhibitor, PF-3758309 (PAK4 IC_{50} = 19 nM, PAK1 IC_{50} = 14 nM), has been advanced to clinical development [13]. PF-3758309 inhibits the growth of many tumour cell lines and has shown potent anticancer properties in xenografts and in a KRAS-driven transgenic mouse model of skin cancer [13,14]. This compound progressed to phase I clinical trials in patients with advanced/metastatic solid tumours, but these clinical trials were halted due to low oral bioavailability (~1%) and adverse events [15]. Compound **2** (GEN-2861), a highly potent group II PAK-selective inhibitor with exquisite kinome selectivity, was reported by Genentech [16]. This compound has been used as a tool compound to evaluate group II PAK biology. Nonetheless, an obstacle to its use is its poor cellular activity. Recently, a few PAK4 small molecule inhibitors have been reported in the literature with diverse

* Corresponding author.
** Corresponding author. Department of Cell Biology, Key Laboratory of Cell Biology, Ministry of Public Health, China Medical University, Shenyang 110001, China.
*** Corresponding author.
E-mail addresses: dongmeiz-67@163.com (D. Zhao), fli@mail.cmu.edu.cn (F. Li), mscheng@263.net (M. Cheng).
[1] These authors contributed equally to this work.

http://dx.doi.org/10.1016/j.ejmech.2017.02.063
0223-5234/

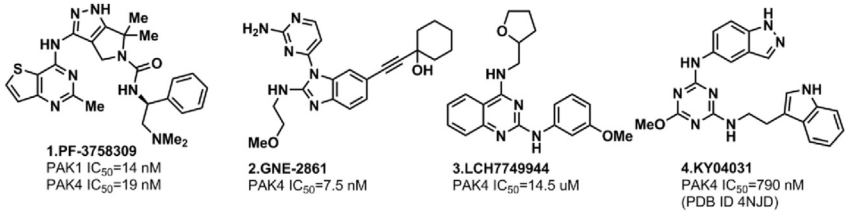

Fig. 1. Known PAK4 inhibitors.

chemotypes and affinities [17–19]. There is a growing need for novel and potent PAK4 inhibitors that can be developed into therapeutic candidates for cancer treatment.

Previously, we described the discovery of anilinoquinazoline PAK4 inhibitor **3** (LCH-7749944) as a moderate PAK4 inhibitor using HTS screening in 2012 [20]. Recently, Ryu et al. reported the discovery of the 1, 3, 5-triazine-based PAK4 inhibitor KY04031 by high throughput HTRF-based screening [21]. This compound inhibits PAK4 kinase with moderate activity (PAK4 IC_{50} = 0.790 μM). A co-crystal structure of KY04031 with PAK4 showed that the indole and indazole rings provide three hydrogen bonds to the kinase hinge region and the triazine moiety enters a lipophilic phosphate-binding pocket (Fig. 2) [21]. However, only this compound was reported, thereby leaving this chemotype largely unexplored. Compound **2** does not fully occupy the large and flexible ATP-binding cleft of PAK4, so we hypothesize that extending the scaffold of **2** into the hydrophobic subsite would provide an opportunity to increase its potency against PAK4. In an attempt to design compounds with enhanced potency against the kinase activity of PAK4, we explored the heterocyclic core using bicyclic systems, intending to induce an interaction with the phosphate-binding region of the ATP-binding pocket (Fig. 3).

This paper describes the design, synthesis, biological evaluation, and molecular modeling of 2, 4-diaminoquinazoline derivatives as potent PAK4 inhibitors. These compounds potently suppressed the enzyme activity, and structure-activity relationships are determined. The most potent compound, **9d,** inhibited PAK4 kinase activity with an IC_{50} value of 0.033 μM, which was 24-fold greater than that of KY04031. Furthermore, compound **9d** inhibited the PAK4-driven cell proliferation in a dose-dependent manner. In addition, mechanistic studies demonstrate that compound **9d** inhibits the migration and invasion of A549 cells via regulation of the PAK4-LIMK1 signalling pathway. A molecular modeling study of compound **9d** was performed to elucidate its possible binding modes and to provide a structural basis for the further structure-guided design of PAK4 inhibitors.

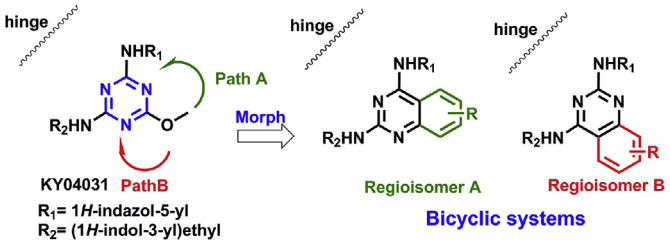

Fig. 3. Core refinement strategy for the development of a novel series of PAK4 inhibitors.

2. Chemistry

The synthesis of the 2, 4-diaminoquinazoline scaffold is described in Scheme 1. Starting from substituted 2,4-dichloroquinazolines **5a-g**, the first chlorine was displaced by nucleophilic substitution with 1*H*-indazol-5-amine at 0 °C to produce the mono-substituted intermediates **6a-g**. The displacement of the second chlorine by tryptamine was accomplished by an HCl-catalysed amination procedure, affording compounds **7a-g** in good yields. Likewise, the second series of 2, 4-diaminoquinazoline regioisomers **9a-g** were synthesized from compounds **5a-g** in a modified reaction sequence.

To study the structure and activity relationship (SAR) of the indazole ring, some of the required hinge-binding moieties (e.g., **13, 17a-b** and **23**) were not commercially available and were prepared as follows. As shown in Scheme 2, (*Z*)-2, 3-dibromo-4-oxobut-2-enoic acid **10** was treated with $NaNO_2$ in ethanol to give compound **11,** which was then converted to **12** by condensation with 1*H*-pyrazol-3-amine according to a literature procedure [22]. Subsequent reduction of the nitro group of **12** afforded heteroaryl amine **13**. As shown in Scheme 3, halogenation of 2-methyl-4-nitroaniline **14** in the presence of NCS or NBS gave halogenated aryls **15a-b,** which were cyclized and reduced to afford **17a** and **17b**.

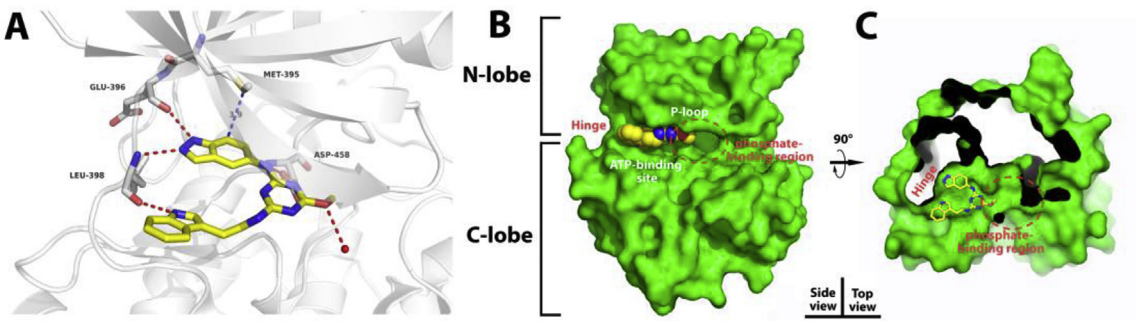

Fig. 2. (A). X-ray crystal structure of the reported 1, 3, 5-triazine inhibitor KY04031 bound to PAK4 (PDB code 4NJD) [21]. Note that C-7 of the indazol ring interacts with the gatekeeper residue Met395. (B). Space-filling diagram of the co-crystal structure of PAK4 with KY04031, highlighting the solvent accessibility of KY04031. Ample space is available within the ATP-binding site allowing for the possibility of a ring fusion to form a quinazoline core, and highlighted by a dashed red oval. (C). Rotated relative to (B). (For interpretation of the references to colour in this figure legend, the reader is referred to the web version of this article.)

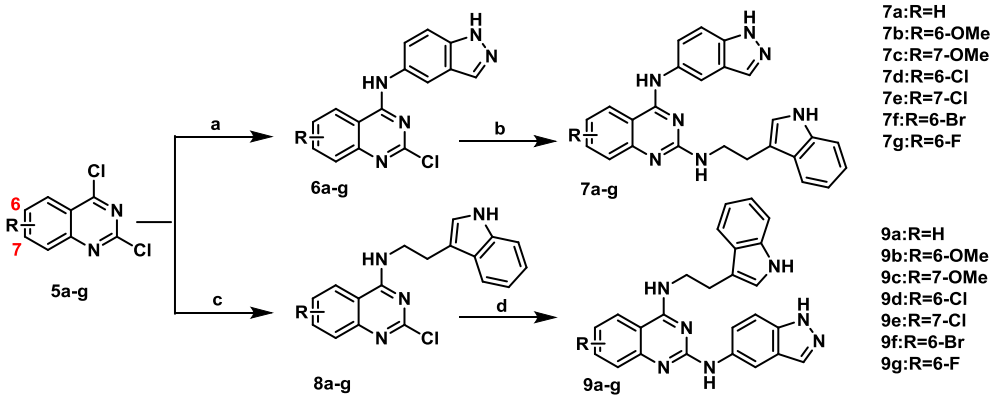

Scheme 1. Reagents and conditions: (a) 1*H*-indazol-5-amine, DIEA, DMF, 0 °C, 2 h (b) tryptamine, HCl, EtOH, 120 °C, 6 h (c) tryptamine, DIEA, DMF, 0 °C, 2 h (d) 1*H*-indazol-5-amine, HCl, EtOH, 120 °C, 6 h.

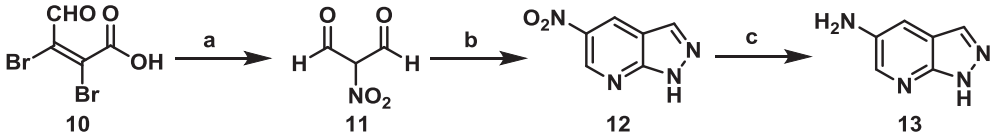

Scheme 2. Reagents and conditions: (a) $NaNO_2$, H_2O, EtOH, 54 °C, 1 h (b) 1*H*-pyrazol-3-amine, H_2O, 90 °C, 16 h (c) H_2, MeOH, Pd/C, r.t, 16 h.

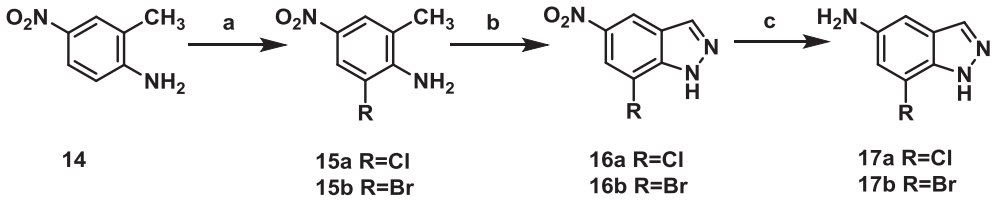

Scheme 3. Reagents and conditions: (a) CH_3CN, NH_4OAc, NCS or NBS, 60 °C, 3 h (b) AcOH, $NaNO_2$, H_2O, r.t, 12 h (c) $SnCl_2$, EtOH, reflux, 18 h.

Similarly, methyl substituted analogue **23** was prepared from 2, 6-dimethylaniline (Scheme 4). Finally, S_NAr displacement of aryl chloride **8d** by various amines afforded the corresponding target compounds **24a-h** (Scheme 5).

3. Results and discussion

3.1. In vitro activity against PAK4 kinase

PAK4 inhibitory activities of the designed compounds **7a-g**, **9a-g** and **24a-h** were preliminarily evaluated via a well-established homogeneous time-resolved fluorescence (HTRF) assay according to the manufactory's instructions (Cisbio). The results are shown in Tables 1 and 2. The well-characterized PAK4 inhibitors PF3758309 and staurosporine were included as positive controls to validate the screening conditions. Under the experimental conditions, both of these compounds displayed strong inhibition against PAK4 with IC_{50} values of 7.0 and 1.9 nM, respectively, which are similar to the previously reported data [11].

As shown in Table 1, a comparison of the A and B regioisomers of

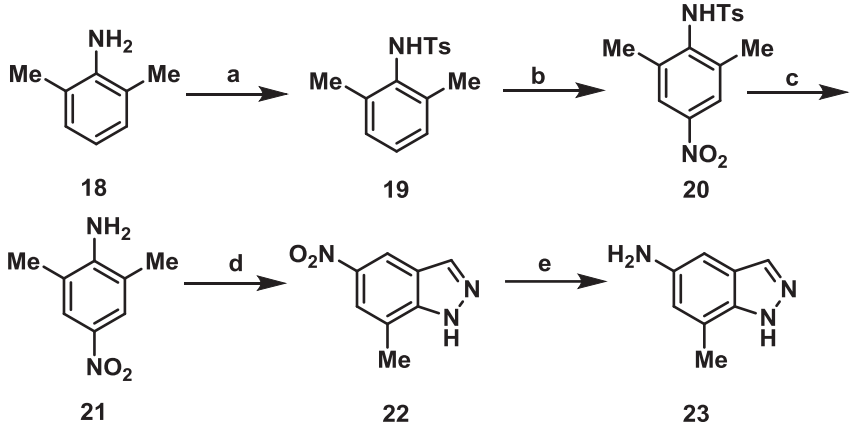

Scheme 4. Reagents and conditions: (a) p-TsCl, pyridine, r.t. (b) HNO_3, AcOH, $NaNO_2$, H_2O, reflux. 4 h. (c) H_2SO_4, 50 °C, 1 h (d) AcOH, $NaNO_2$, H_2O, r.t. 12 h. (e) H_2, Pd-C, MeOH, r.t, 12 h.

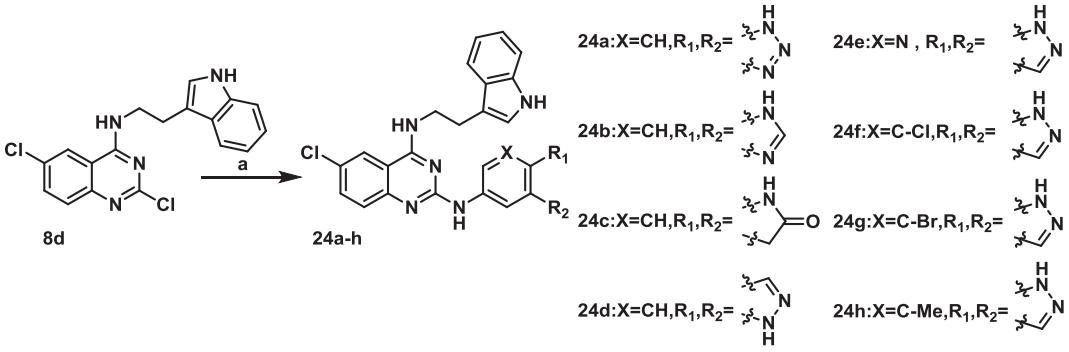

Scheme 5. Reagents and conditions: (a) amine, HCl, EtOH, 120 °C, 6 h.

the 2,4-diaminoquinazoline derivatives (**7a-g** and **9a-g)** revealed that, in general, the B regioisomer is a more active PAK4 inhibitor. For example, compound **9a** (IC_{50} = 0.406 μM) showed 8.7-fold higher affinity to PAK4 than **7a** (IC_{50} = 3.516 μM). Morphing from the triazine core to a quinazoline resulted in a clear increase in PAK4 inhibition activity (**9a**, IC_{50} = 0.46 μM), compared to the 1,3,5-triazinic lead compound KY04031 (IC_{50} = 0.79 μM), suggesting a specific contribution by the quinazoline heterocyclic core. We further investigated the impact of quinazoline ring substitution on PAK4 inhibitory activity and found that the position of the substituent on the ring significantly affected the biological activity of the resulting compounds. Among the substituents at the C-6 position of the quinazoline core, the 6-Cl substituted derivative **9d** demonstrated the greatest potency (IC_{50} = 0.033 μM). Chlorine atom substitution of the C-7 position led to a loss of potency (**9e**, IC_{50} = 0.360 μM). Further investigation showed that the 6-chloro group in **9d** could be replaced by 6-Br (**9f**) or 6-F (**9g**) and PAK4 inhibitory activity was retained, but the potency decreased.

To further study the relationship between the indazol ring and PAK4 inhibition, additional compounds, **24a-h**, were prepared, based on compound **9d** and evaluated for their activity (Table 2). As mentioned above, the indazol ring makes a two-point interaction with Leu398 and Glu396 in the hinge region. Rearrangement of the donor-acceptor array on the indazol ring led to a loss of potency (**24a-d**), highlighting the necessity of the hydrogen bond donor and acceptor in this region.

As observed in the PAK4-compound **4** co-crystal structure (PDB ID 4NJD, Fig. 2), C-7 of the indazol ring interacts with the gatekeeper residue Met395. Compound **24e-h** were synthesized to probe the effects of substitution on the inhibitory potency of PAK4. Compounds with C-H (**9d**), N (**24e**), C-Cl (**24f**), C-Br (**24g**), and C-methyl (**24h**) at the 7 position of indazole ring displayed IC_{50} values of 0.033, 0.63, 0.94, 1.06, and 2.33 μM, respectively. As the size of the C7-substituents increased from H to Cl to Br and CH_3, the

Table 1
In vitro enzymatic activities of isomeric 2,4-diaminoquinazoline derivatives **7a-g** and **9a-g**.

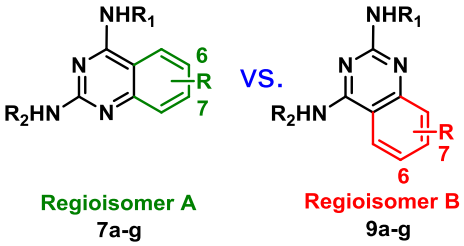

No.	R	R_1	R_2	Regioisomer	IC_{50} (μM)[a,b]
7a	H	1*H*-indazol-5-yl	(1*H*-indol-3-yl)ethyl	A	3.516
7b	6-OMe	1*H*-indazol-5-yl	(1*H*-indol-3-yl)ethyl	A	1.709
7c	7-OMe	1*H*-indazol-5-yl	(1*H*-indol-3-yl)ethyl	A	3.956
7d	6-Cl	1*H*-indazol-5-yl	(1*H*-indol-3-yl)ethyl	A	0.093
7e	7-Cl	1*H*-indazol-5-yl	(1*H*-indol-3-yl)ethyl	A	4.470
7f	6-Br	1*H*-indazol-5-yl	(1*H*-indol-3-yl)ethyl	A	0.788
7g	6-F	1*H*-indazol-5-yl	(1*H*-indol-3-yl)ethyl	A	1.736
9a	H	(1*H*-indol-3-yl)ethyl	1*H*-indazol-5-yl	B	0.406
9b	6-OMe	(1*H*-indol-3-yl)ethyl	1*H*-indazol-5-yl	B	1.506
9c	7-OMe	(1*H*-indol-3-yl)ethyl	1*H*-indazol-5-yl	B	0.483
9d	6-Cl	(1*H*-indol-3-yl)ethyl	1*H*-indazol-5-yl	B	0.033
9e	7-Cl	(1*H*-indol-3-yl)ethyl	1*H*-indazol-5-yl	B	0.360
9f	6-Br	(1*H*-indol-3-yl)ethyl	1*H*-indazol-5-yl	B	0.177
9g	6-F	(1*H*-indol-3-yl)ethyl	1*H*-indazol-5-yl	B	0.920
1[c]	–	–	–	–	0.007
Staurosporine[c]	–	–	–	–	0.0019

[a] IC_{50} values are calculated based on the homogeneous time-resolved fluorescence (HTRF) assay.
[b] Reported data are the mean values from two independent experiments.
[c] Used as a positive control.

Table 2
SAR of the indazol ring.

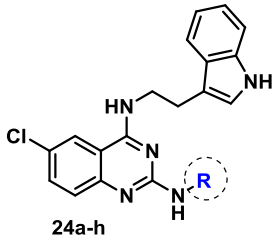

24a-h

No.	R	IC_{50} (μM)[a,b]	No.	R	IC_{50} (μM)[a,b]
24a	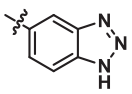	1.163	**24e**	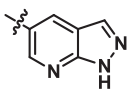	0.633
24b	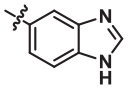	3.071	**24f**	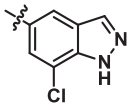	0.937
24c	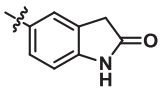	1.757	**24g**		1.056
24d	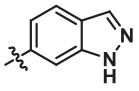	2.040	**24h**	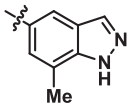	2.334
9d	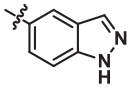	0.033	**1**[c]	–	0.007

[a] IC_{50} values are calculated based on the homogeneous time-resolved fluorescence (HTRF) assay.
[b] Reported data are the mean values from two independent experiments.
[c] Used as a positive control.

activity against PAK4 gradually decreased. The X-ray crystal structure of **4** in PAK4 indicates that the distance between the C7 atom of the indazol ring and Met395 is 3.9 Å ($d_{C\text{-}7 \ldots S}$), which is approximately the sum of van der Waals radii of both atoms. This compact packing might explain why groups with larger van der Waals radii, such as chlorine (**24f**), bromine (**24g**) or methyl (**24h**), are not well-tolerated at this position. These results confirmed that compound **9d** binds in the ATP binding site with C-7 of the indazol ring interacting with the gatekeeper residue Met395.

3.2. Molecular docking study of compound *9d*

In an attempt to gain insight into the putative binding mode of optimized inhibitor **9d** with the PAK4 kinase compared to the lead compound KY04031, molecular docking of this compound into the ATP binding site of the PAK4 kinase (PDB ID 4NJD) was performed. The program AutoDock 4 with default parameters was used to perform this simulation. The resulting binding mode of compound **9d** is depicted in Fig. 4. As expected, compound **9d** is able to bind to the ATP-binding site of PAK4 in a similar way as KY04031, sandwiched in a narrow cleft formed by the C and N lobes. The three hydrogen bonds to the kinase hinge region (i.e., residues, Glu396 and Leu398) made by the indole and indazole rings of KY04031 are conserved in the docked pose of **9d**. The N^4-N*H* of the quinazoline core leads to a hydrogen bond contact with the neighboring charged residue Asp458 (DFG-motif). Compared to KY04031, the bulkier quinazoline core of **9d** addresses the lipophilic phosphate-binding pocket to a greater degree than the triazine core of compound **4**, making hydrophobic contact with Val335. These hydrogen-bond interactions, together with the interactions made by the quinazoline ring, may be responsible for the increased the binding affinity of **9d** to compared to KY04031.

3.3. Compound *9d* induces cell cycle arrest in G2/M phase

PAK4 is an important oncogene whose expression is increased in various human cancers, and many of its functions are dependent on its kinase activity. Based on the enzymatic assay results, we tested the ability of compound **9d** to inhibit the growth of the PAK4-dependent tumour cell line A549 (human lung adenocarcinoma) [8] and cell line. Meanwhile, the tumour cell line NCI-H460 (human large cell lung cancer cell) [24], whose growth was not dependent on PAK4, was used to test the potential off-target effects. The cytotoxicity in HEK-293 cells (human embryonic kidney 293 cell) was determined as an indicator of toxicity. In the MTT assay, compound **9d** inhibited the proliferation of A549 cells in a concentration-dependent manner (Fig. 5A). Of note, the weak cytotoxicity in HEK-293 cells suggested the potential safety of compound **9d**. Next, we determined whether the **9d**-induced decrease in PAK4 phosphorylation would result in cell cycle arrest in the A549 cell line. Cell cycle analysis was performed using flow cytometry (Fig. 5B). When A549 cells were treated with **9d** at 1 μM or 5 μM, the number of cells in the G1 phase increased from 73.42% to 73.57% and 84.43%, whereas cells in the S phase decreased from 19.83% to 19.71% and 10.98%, respectively, compared with the controls. To further dissect the molecular mechanisms underlying the cell proliferation regulation, we investigated the expression of some genes related to cell cycle progression. Western blot analysis showed that exposure of the A549 cells to 10 μmol/L **9d** for 24 h markedly increased protein expression of CDK inhibitors (p21, p18) and decreased the protein expression of cyclin D3 and CDK6 (Fig. 5C). This result indicates that **9d** arrested cells at the G1 phase in a PAK4 kinase-dependent manner, as a result, suppressed lung adenocarcinoma cell growth via cyclin D3 and CDK6.

3.4. Effect of compound *9d* on cell migration and invasion

Metastasis is a multistep process that results from the convergence of a variety of cellular processes. These processes include cell migration, invasion, adhesion to the surrounding stroma and through vessel walls, and survival in a foreign environment. As previously mentioned, PAK4 is critical for migration and invasion. The inhibitory effects of **9d** on cell migration and invasion of A549 cells cancer cell lines were analysed using a Transwell assay (with or without Matrigel) [25]. As shown in Fig. 6A and B, in A549 cells, a dose-dependent decrease in cell migration and invasion was observed following treatment with compound **9d**.

Previous studies showed that LIMK and its downstream cofilin activated by PAK4. This pathway plays an important role in promoting actin polymerization and defining the direction of cell motility [26]. To further illustrate the mechanism of our compound with respect to these effects, we investigated the effects of compound **9d** on the PAK4/LIMK1/cofilin signalling pathway by western blot analysis. As expected, exposure of A549 cells to different concentrations of compound **9d** for 24 h inhibited the levels of activated PAK4 ($PAK4^{p-Ser474}$) [27] and phosphor-LIMK1 ($LIMK^{p-Thr508}$) [28] in a dose-dependent manner (Fig. 6C), indicating that the mechanism of **9d** repressing breast cancer cell migration and invasion correlates with **9d** inhibiting PAK4 kinase activity and its downstream substrates.

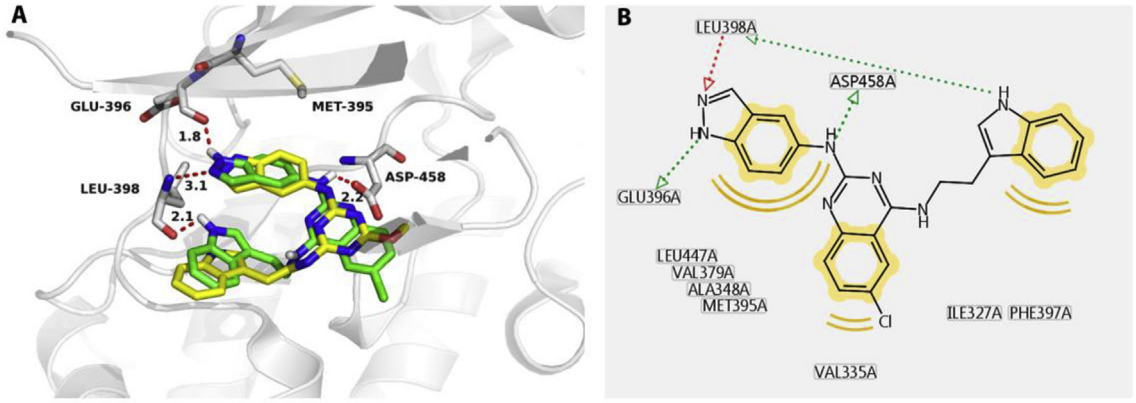

Fig. 4. Predicted binding mode of **9d** in the ATP-binding site of PAK4. (A). Overlay of **9d** (green) and lead compound **4** (KY04031, yellow) bound in the kinase active site (PDB code 4NJD for KY04031). The bulkier quinazoline core of **9d** addresses the lipophilic phosphate-binding pocket to a greater degree than the triazine core of compound **4.** Hydrogen bond distances are in Å. (B). Compound **9d** interaction diagram (2D representation) by LigandScout software [23]. (For interpretation of the references to colour in this figure legend, the reader is referred to the web version of this article.)

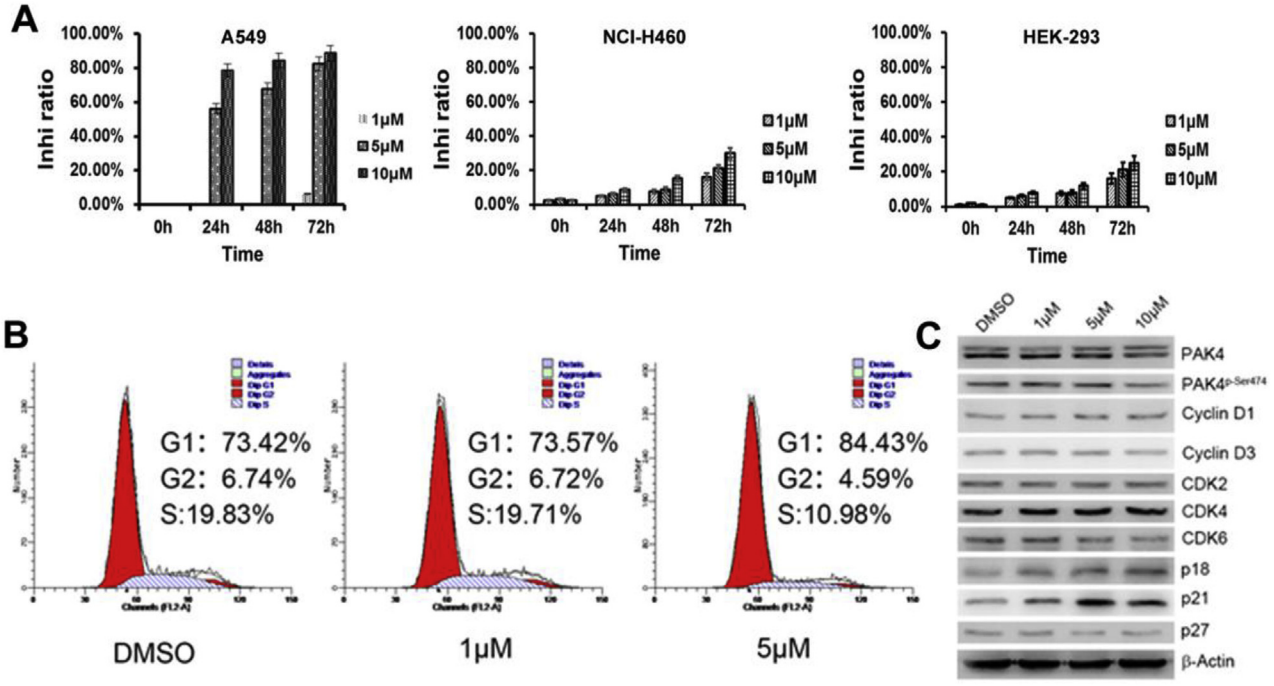

Fig. 5. Compound **9d** affects the cell cycle distribution in A549 cancer cells. (A) A549, NCI-H460, and HEK-293 cells were cultured with the indicated concentrations of compound **9d** for the indicated hours. Compound **9d** suppresses the proliferation of lung adenocarcinoma cells. (B) Untreated cells (control) and cells treated for 24 h with different concentrations of compound **9d**. (C) Proteins from the cells in (B) were extracted to examine the expression of the indicated proteins by western blot analysis. Compound **9d** up-regulates the expression levels of CDK inhibitors (p21, p18) and down-regulates the expression levels of PAK4$^{p-Ser474}$, cyclin D3, and CDK6.

4. Conclusions

In summary, based on a scaffold morphing strategy and structure-guided SAR design, we developed a series of 2,4-diaminoquinazoline derivatives as a new class of PAK4 inhibitors. The compounds potently suppressed the enzymatic activities of PAK4 with IC_{50} values in the 10^{-6}-10^{-8} M range. SAR and biological evaluations of this series of compounds were discussed. The optimized compound **9d** suppressed the proliferation of human A549 cancer cells, in which PAK4 expression was high. Furthermore, compound **9d** potently suppressed cancer cell migration and invasion, indicating its potential to serve as a new lead compound for further anticancer drug discovery.

5. Experimental

5.1. Chemistry

^{1}H NMR and ^{13}C NMR spectral data were recorded in $CDCl_3$ or DMSO-d_6 on Bruker ARX-400 NMR or Bruker ARX-600 NMR spectrometers. High resolution accurate mass spectrometry determinations (HRMS) for all final target compounds were obtained on a Bruker Micromass Time of Flight mass spectrometer equipped with an electrospray ionisation (ESI) detector. Unless otherwise noted, all commercial reagents and solvents were purchased from vendors and were used without further purification or distillation. All tested compounds had a purity ≥95%. Column chromatography

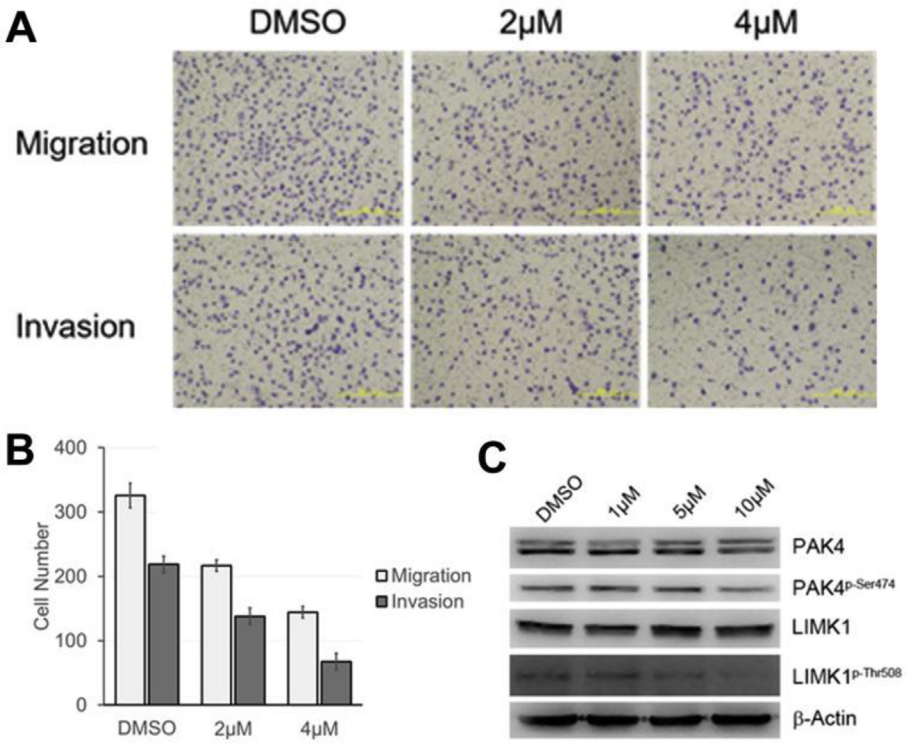

Fig. 6. Compound **9d** suppresses the migration and invasion of A549 cells and inhibits the PAK4/LIMK1 pathways. (A) (B) The migratory and invasive capacities of A549 cells were evaluated using a Transwell assay (with or without Matrigel). After 24 h of treatment with the indicated concentrations of compound **9d**, the invaded cells were fixed and stained and 10 random fields were counted. (C) Western blot analysis showing the protein level of the proteins involved in migration and invasion. Compound **9d** inhibited the levels of activated PAK4 and phosphor-LIMK1 in a dose-dependent manner.

was carried out on silica gel (200–300 mesh). All reactions were monitored using thin layer chromatography (TLC) on silica gel plates.

*5.1.1. Representative procedure for the synthesis of N^2-(2-(1H-indol-3-yl)ethyl)-N^4-(1H-indazol-5-yl)quinazoline -2,4-diamine (**7a**)*

*5.1.1.1. 2-Chloro-N-(1H-indazol-5-yl)quinazolin-4-amine (**6a**).* To a flask charged with 2, 4-dichloroquinazoline (**5a**, 0.20 g, 1 mmol) was added DMF (5 mL) and DIEA (0.17 mL, 3 mmol). The mixture was cooled in an ice water bath prior to the addition of 1*H*-indazol-5-amine (0.15 g, 1.1 mmol). The reaction mixture was stirred at 0 °C. After completion of the reaction (as determined by TLC analysis), the mixture was poured into ice-cold water. The resulting solid was collected on a glass filter to give the crude product. The filtrate was subjected to silica gel column chromatography using dichloromethane/acetone (15:1) as the mobile phase to afford the compound **6a** as a pale-yellow solid (168 mg, 0.57 mmol, 57% yield). Mp: decomp. above 300 °C. Rf: 0.40 (DCM/MeOH, 15/1, v/v). ^{1}H NMR (400 MHz, DMSO-d_6): 13.16 (s, 1H), 10.31 (s, 1H), 8.58 (d, J = 8.2 Hz, 1H), 8.14 (s, 1H), 8.10 (s, 1H), 7.88 (t, J = 8.0 Hz, 1H), 7.71 (d, J = 8.1 Hz, 1H), 7.67–7.60 (m, 3H). MS (ESI$^+$) *m/z*: 295.9 $[M+H]^+$, 318.0 $[M+Na]^+$.

*5.1.1.2. N^2-(2-(1H-indol-3-yl)ethyl)-N^4-(1H-indazol-5-yl)quinazoline-2,4-diamine (**7a**).* To a vessel charged with 2-chloro-*N*-(1*H*-indazol-5-yl)quinazolin-4-amine (**6a**, 168 mg, 0.57 mmol) was added ethanol(5 mL), hydrochloric acid (10 μL), and tryptamine (91 mg, 0.57 mmol). The vessel was sealed and stirred for 6 h at 120 °C. The resulting mixture was dried under reduced pressure and subjected to silica gel column chromatography using DCM/methanol (90:10) as mobile phase to afford the desired compound **7a** as white solid (103 mg, 43%). Mp: decomp. above 265 °C. Rf: 0.20 (DCM/MeOH, 10/1, v/v). ^{1}H NMR (400 MHz, DMSO-d_6): 13.22 (s, 1H), 12.88 (br, 1H), 11.04–10.70 (m, 2H), 8.64–8.63 (m, 1H), 8.18–8.09 (m, 2H), 7.92–7.82 (m, 2H), 7.64–7.45 (m, 4H), 7.33–7.28 (m, 2H), 7.03–6.75 (m, 3H), 3.75–3.59 (m, 2H), 3.03–2.92 (m, 2H). ^{13}C NMR (100 MHz, DMSO-d_6): 159.4, 153.7, 140.2, 138.5, 136.7, 135.8, 134.2, 130.3, 127.5, 125.2, 124.6, 123.3, 123.0, 121.4, 118.7, 117.4, 116.2, 111.8, 111.5, 110.5, 42.0, 25.6. HRMS (ESI$^+$): *m/z* calcd for $C_{25}H_{21}N_7$, 420.1931, found, 420.1933.

*5.1.2. N^2-(2-(1H-indol-3-yl)ethyl)-N^4-(1H-indazol-5-yl)-6-methoxyquinazoline-2,4-diamine (**7b**)*

Following the general procedure mentioned above, using **5b** (0.23 g, 1 mmol) as the starting material, compound **7b** was obtained as a light yellow solid (99 mg, 22%, two steps). Mp: 265–268 °C. Rf: 0.17 (DCM/MeOH, 10/1, v/v). ^{1}H NMR (400 MHz, DMSO-d_6): 13.21 (s, 1H), 12.65 (br, 1H), 10.99–10.73 (m, 2H), 8.13–7.70 (m, 4H), 7.66–7.50 (m, 4H), 7.33–7.24 (m, 2H), 7.03–6.77 (m, 3H), 3.92 (s, 3H), 3.68–3.58 (m, 2H), 3.01–2.91 (m, 2H). ^{13}C NMR (100 MHz, DMSO-d_6): 159.1, 156.5, 152.9, 138.6, 136.6, 134.2, 130.3, 127.5, 124.8, 121.4, 118.7, 116.4, 111.8, 111.5, 110.5, 106.2, 56.7, 42.1, 25.6. HRMS (ESI$^+$): *m/z* calcd for $C_{26}H_{23}N_7O$, 450.2037, found, 450.2034.

*5.1.3. N^2-(2-(1H-indol-3-yl)ethyl)-N^4-(1H-indazol-5-yl)-7-methoxyquinazoline-2,4-diamine (**7c**)*

Following the general procedure mentioned above, using **5c** (0.23 g, 1 mmol) as the starting material, compound **7c** was obtained as a white solid (117 mg, 26%, two steps). Mp: 299–300 °C. Rf: 0.28 (DCM/MeOH, 10/1, v/v). ^{1}H NMR (400 MHz, DMSO-d_6): 13.17 (s, 1H), 12.68 (br, 1H), 10.86–10.48 (m, 2H), 8.54–8.49 (m, 1H), 8.49–7.90 (m, 3H), 7.61–7.51 (m, 2H), 7.32–7.26 (m, 2H), 7.08–6.77

(m, 4H), 3.90 (s, 3H), 3.72–3.57 (m, 2H), 3.02–2.91 (m, 2H). ^{13}C NMR (100 MHz, DMSO-d_6): 164.9, 159.0, 153.7, 142.4, 138.4, 136.7, 134.1, 130.4, 127.5, 127.1, 124.6, 123.3, 123.0, 121.4, 118.7, 116.1, 113.9, 111.8, 111.5, 110.4, 103.9, 99.3, 42.0, 25.6. HRMS (ESI$^+$): *m*/*z* calcd for $C_{26}H_{23}N_7O$, 450.2037, found, 450.2051.

5.1.4. N^2-(2-(1H-indol-3-yl)ethyl)-6-chloro-N^4-(1H-indazol-5-yl) quinazoline-2,4-diamine (**7d**)

Following the general procedure mentioned above, using **5d** (0.23 g, 1 mmol) as the starting material, compound **7d** was obtained as an off-white solid (191 mg, 42%, two steps). Mp: 245–246 °C. Rf: 0.28 (DCM/MeOH, 10/1, v/v). ^{1}H NMR (100 MHz, DMSO-d_6): 13.02 (s, 1H), 10.81 (s, 1H), 9.67–9.49 (m, 1H), 8.48 (d, J = 2.0 Hz, 1H), 8.37 (s, 1H), 8.04 (s, 1H), 7.70 (dd, J = 1.4, 8.9 Hz, 1H), 7.58 (dd, J = 2.0, 8.9 Hz, 1H), 7.53 (s, 1H), 7.38 (s, 1H), 7.34 (d, J = 8.2 Hz, 1H), 7.18–7.00 (m, 4H), 3.64–3.59 (m, 2H), 3.00–2.96 (m, 2H). ^{13}C NMR (400 MHz, DMSO-d_6):159.5, 158.1, 151.4, 157.6, 136.7, 133.9, 133.2, 132.7, 127.8, 124.6, 123.6, 123.3, 123.0, 122.8, 121.3, 119.8, 118.6, 113.5, 112.7, 111.8, 110.2, 42.1, 25.7. HRMS (ESI$^+$): *m*/*z* calcd for $C_{25}H_{20}ClN_7$, 454.1541, found, 454.1542.

5.1.5. N^2-(2-(1H-indol-3-yl)ethyl)-7-chloro-N^4-(1H-indazol-5-yl) quinazoline-2,4-diamine (**7e**)

Following general the procedure mentioned above, using **5e** (0.23 g, 1 mmol) as the starting material, compound 7**e** was obtained as a white solid (163 mg, 36%, two steps). Mp: 298–301 °C. Rf: 0.28 (DCM/MeOH, 10/1, v/v). ^{1}H NMR (400 MHz, DMSO-d_6): 13.22 (s, 1H), 12.89 (br, 1H), 11.11–10.81 (m, 2H), 8.66–8.60 (m, 1H), 8.34–7.92 (m, 3H), 7.62–7.53 (m, 4H), 7.33–7.28 (m, 2H), 7.06–6.75 (m, 3H), 3.78–3.58 (m, 2H), 3.04–2.91 (m, 2H). ^{13}C NMR (100 MHz, DMSO-d_6): 158.9, 153.5, 141.1, 140.1, 138.5, 136.6, 134.2, 130.1, 127.5, 127.3, 124.8, 124.6, 124. 4, 123.3, 123.0, 121.4, 118.7, 116.6, 116.2, 111.8, 111.4, 110.5, 109.4, 42.1, 25.5. HRMS (ESI$^+$): *m*/*z* calcd for $C_{25}H_{20}ClN_7$, 454.1541, found, 454.1564.

5.1.6. N^2-(2-(1H-indol-3-yl)ethyl)-6-bromo-N^4-(1H-indazol-5-yl) quinazoline-2,4-diamine (**7f**)

Following general the procedure mentioned above, using **5f** (0.28 g, 1 mmol) as the starting material, compound **7f** was obtained as a white solid (195 mg, 39%, two steps). Mp: decomp. above 284 °C. Rf: 0.28 (DCM/MeOH, 10/1, v/v). ^{1}H NMR (400 MHz, DMSO-d_6): 13.23 (s, 1H), 13.07 (br, 1H), 11.03 (s, 1H), 10.89 (s, 1H), 8.93–8.87 (m, 1H), 8.27–8.23 (m, 1H), 8.11 (s, 1H), 8.00–7.91 (m, 1H), 7.65–7.27 (m, 6H), 7.13–6.76 (m, 3H), 3.75–3.60 (m, 2H), 3.03–2.93 (m, 2H). ^{13}C NMR (100 MHz, DMSO-d_6): 158.3, 153.8, 138.5, 138.2, 136.7, 134.1, 130.3, 127.5, 124.2, 123.3, 123.0, 121.4, 120.0, 118.7, 116.1, 115.9, 112.1, 111.8, 111.5, 110.5, 42.1, 25.6. HRMS (ESI$^+$): *m*/*z* calcd for $C_{25}H_{20}BrN_7$, 500.1016, found, 500.1019.

5.1.7. N^2-(2-(1H-indol-3-yl)ethyl)-6-fluoro-N^4-(1H-indazol-5-yl) quinazoline-2,4-diamine (**7g**)

Following the general procedure mentioned above, using **5g** (0.22 g, 1 mmol) as the starting material, compound **7g** was obtained as a white solid (118 mg, 27%, two steps). Mp: decomp. above 262 °C. Rf: 0.28 (DCM/MeOH, 10/1, v/v). ^{1}H NMR (400 MHz, DMSO-d_6): 13.20 (s, 1H), 12.77 (br, 1H), 10.88 (s, 2H), 8.53–8.47 (m, 1H), 8.25–8.13 (m, 2H), 7.90–7.60 (m, 2H), 7.66–7.57 (m, 3H), 7.34–7.25 (m, 2H), 7.05–6.79 (m, 2H), 3.70–3.62 (m, 2H), 3.02–2.94 (m, 2H). ^{13}C NMR (100 MHz, DMSO-d_6): 158.9, 154.3, 138.3, 136.7, 134.1, 130.6, 127.6, 124.2, 123.3, 123.1, 121.4, 118.7, 115.7, 111.8, 110.5, 42.1, 25.6. HRMS (ESI$^+$): *m*/*z* calcd for $C_{25}H_{20}FN_7$, 438.1837, found, 438.1826.

5.1.8. Representative procedure for the synthesis of N4-(2-(1H-indol-3-yl)ethyl)-N2-(1H -indazol-5-yl)quinazoline -2,4-diamine (**9a**)

5.1.8.1. N-(2-(1H-indol-3-yl)ethyl)-2-chloroquinazolin-4-amine (**8a**).

To a flask charged with 2, 4-dichloroquinazoline (**5a**, 0.20 g, 1.0 mmol) was added DMF (5 mL) and DIEA (0.17 mL, 1.5 mmol). The mixture was cooled in an ice water bath prior to the addition of tryptamine (0.18 g, 1.1 mmol). The reaction mixture was stirred at 0 °C. After completion of the reaction (as determined by TLC analysis), the mixture was poured into ice-cold water. The resulting solid was collected on a glass filter to give the crude product. The filtrate was subjected to silica gel column chromatography using dichloromethane/acetone (15:1) as mobile phase to afford the compound **8a** as a pale-yellow solid (232 mg, 0.72 mmol, 72% yield). Mp: 171–172 °C. Rf: 0.60 (DCM/MeOH, 15/1, v/v). ^{1}H NMR (400 MHz, DMSO-d_6): 10.85 (s, 1H), 8.94 (t, J = 5.4 Hz, 1H), 8.25 (d, J = 8.0 Hz, 1H), 7.82–7.78 (m, 1H), 7.72 (d, J = 7.8 Hz, 1H), 7.64 (d, J = 8.0 Hz, 1H), 7.56–7.52 (m, 1H), 7.35 (d, J = 8.1 Hz, 1H), 7.22 (d, J = 2.0 Hz, 1H), 7.05 (t, J = 7.1 Hz, 1H), 6.99 (d, J = 7.3 Hz, 1H), 3.81–3.76 (m, 2H), 3.12–3.06 (m, 2H). MS (ESI$^+$) *m*/*z*: 323.1[M+H]$^+$.

5.1.8.2. N^4-(2-(1H-indol-3-yl)ethyl)-N^2-(1H-indazol-5-yl)quinazoline-2,4-diamine (**9a**).

To a vessel charged with *N*-(2-(1*H*-indol-3-yl)ethyl)-2-chloroquinazolin-4-amine (**8a**, 232 mg, 0.72 mmol) was added ethanol (5 mL), hydrochloric acid (10 μL), and 1*H*-indazol-5-amine (96 mg, 0.72 mmol). The vessel was sealed and stirred for 6 h at 120 °C. The resulting mixture was dried under reduced pressure and subjected to silica gel column chromatography using dichloromethane/methanol (90:10) as the mobile phase to afford the desired compound **9a** as a white solid (184 mg, 0.87 mmol, 61% yield). Mp: decomp. above 260 °C. Rf: 0.17 (DCM/MeOH, 10/1, v/v). ^{1}H NMR (400 MHz, DMSO-d_6): 13.21 (s, 1H), 12.57 (br, 1H), 10.92 (s, 1H), 10.50 (s, 1H), 10.01 (s, 1H), 8.39 (d, J = 8.1 Hz, 1H), 7.98 (s, 1H), 7.91 (s, 1H), 7.81 (t, J = 7.7 Hz, 1H), 7.55 (d, J = 8.0 Hz, 1H), 7.47–7.43 (m, 3H), 7.35 (d, J = 8.1 Hz, 1H), 7.15 (s, 1H), 7.04 (t, J = 7.3 Hz, 1H), 6.84 (t, J = 7.1 Hz, 1H), 3.86–3.85 (m, 2H), 3.12–3.08 (m, 2H). ^{13} C NMR (100 MHz, DMSO-d_6): 160.4, 152.5, 139.3, 138.4, 136.7, 135.6, 134.0, 129.8, 127.5, 125.0, 124.7, 123.6, 123.4, 123.2, 124.5, 118.7, 117.8, 111.9, 111.7, 111.1, 110.8, 42.8, 24.7. HRMS (ESI$^+$): *m*/*z* calcd for $C_{25}H_{21}N_7$, 420.1931, found, 420.1931.

5.1.9. N^4-(2-(1H-indol-3-yl)ethyl)-N^2-(1H-indazol-5-yl)-6-methoxyquinazoline-2,4-diamine (**9b**)

Following the general procedure mentioned above, using **5b** (0.23 g, 1 mmol) as the starting material, compound **9b** was obtained as a light yellow solid (144 mg, 32%, two steps). Mp: 258–260 °C. Rf: 0.17 (DCM/MeOH, 10/1, v/v). ^{1}H NMR (400 MHz, DMSO-d_6): 13.19 (s, 1H), 12.25 (br, 1H), 10.91 (s, 1H), 10.27 (s, 1H), 9.85 (s, 1H), 7.94 (s, 2H), 7.89 (d, J = 2.4 Hz, 1H), 7.57–7.53 (m, 2H), 7.47–7.41 (m, 3H), 7.35 (d, J = 8.1 Hz, 1H), 7.15 (s, 1H), 7.05 (t, J = 7.3 Hz, 1H), 6.86 (t, J = 7.2 Hz, 1H), 3.87 (s, 3H), 3.85–3.83 (m, 2H), 3.12–3.08 (m, 2H). ^{13} C NMR (100 MHz, DMSO-d_6): 160.1, 156.6, 152.0, 138.3, 136.7, 134.0, 127.6, 125.1, 123.7, 123.4, 123.2, 121.5, 119.4, 118.7, 111.9, 111.8, 111.4, 111.1, 106.0, 56.7, 42.8, 24.7. HRMS (ESI$^+$): *m*/*z* calcd for $C_{26}H_{23}N_7O$, 450.2037, found, 450.2053.

5.1.10. N^4-(2-(1H-indol-3-yl)ethyl)-N^2-(1H-indazol-5-yl)-7-methoxyquinazoline-2,4-diamine (**9c**)

Following the general procedure mentioned above, using **5c** (0.23 g, 1 mmol) as the starting material, compound **9c** was obtained as a white solid (167 mg, 37%, two steps). Mp: decomp. above 288 °C. Rf: 0.20 (DCM/MeOH, 10/1, v/v). ^{1}H NMR (600 MHz, DMSO-d_6): 13.18 (s, 1H), 12.33 (br, 1H), 10.89 (s, 1H), 10.44 (s, 1H), 9.68 (s, 1H), 8.27 (d, J = 9.1 Hz, 1H), 7.97 (s, 1H), 7.91 (s, 1H), 7.55 (d, J = 7.5 Hz, 1H), 7.44–7.42 (m, 2H), 7.34 (d, J = 8.1 Hz, 1H), 7.14 (s, 1H),

7.05–7.03 (m, 2H), 7.00 (s, 1H), 6.85 (m, 1H), 3.87 (s, 3H), 3.83–3.82 (m, 2H), 3.09–3.07 (m, 2H). ^{13} C NMR (100 MHz, DMSO-d_6): 164.6, 160.0, 136.7, 134.0, 127.6, 126.5, 123.2, 121.4, 118.7, 114.2, 111.9, 111.8, 104.3, 99.9, 56.4, 42.6, 24.8. HRMS (ESI$^+$): m/z calcd for $C_{26}H_{23}N_7O$, 450.2037, found, 450.2044.

*5.1.11. N^4-(2-(1H-indol-3-yl)ethyl)-6-chloro-N^2-(1H-indazol-5-yl) quinazoline-2,4-diamine (**9d**)*

Following the general procedure mentioned above, using **5d** (0.23 g, 1 mmol) as the starting material, compound **9d** was obtained as a light yellow solid (249 mg, 55%, two steps). Mp: 289–292 °C. Rf: 0.27 (DCM/MeOH, 10/1, v/v). ^{1}H NMR (400 MHz, DMSO-d_6):13.17 (s, 1H), 12.76 (br, 1H), 10.86 (s, 1H), 10.71 (s, 1H), 9.99 (s, 1H), 8.54 (d, J = 2.0 Hz, 1H), 8.08 (s, 1H), 7.88–7.85 (m, 2H), 7.76 (d, J = 8.6 Hz, 2H), 7.60 (d, J = 8.9 Hz, 1H), 7.45 (d, J = 7.9 Hz, 1H), 7.33 (d, J = 8.1 Hz, 1H), 7.26 (dd, J = 1.3, 8.6 Hz, 1H), 7.14 (d, J = 1.4 Hz, 1H), 7.03 (t, J = 7.4 Hz, 1H), 6.83 (t, J = 7.4 Hz, 1H), 3.91–3.86 (m, 2H), 3.15–3.11 (m, 2H). ^{13} C NMR (100 MHz, DMSO-d_6): 159.6, 152.7, 138.4, 136.7, 135.4, 134.0, 128.8, 127.5, 124.2, 123.3, 121.5, 120.0, 118.7, 118.6, 112.1, 111.9, 111.6, 111.1, 42.9, 24.5. HRMS (ESI$^+$): m/z calcd for $C_{25}H_{20}ClN_7$, 454.1541, found, 454.1550.

*5.1.12. N^4-(2-(1H-indol-3-yl)ethyl)-7-chloro-N^2-(1H-indazol-5-yl) quinazoline-2,4-diamine (**9e**)*

Following the general procedure mentioned above, using **5e** (0.23 g, 1 mmol) as the starting material, compound **9e** was obtained as a yellow solid (231 mg, 51%, two steps). Mp: decomp. above 267 °C. Rf: 0.27 (DCM/MeOH, 10/1, v/v). ^{1}H NMR (400 MHz, DMSO-d_6): 13.23 (s, 1H), 12.62 (br, 1H), 10.91 (s, 1H), 10.56 (s, 1H), 10.02 (s, 1H), 8.39 (d, J = 8.7 Hz, 1H), 7.95 (s, 1H), 7.65 (s, 1H), 7.58–7.52 (m, 2H), 7.44–7.42 (m, 2H), 7.34 (d, J = 8.1 Hz, 1H), 7.15 (s, 1H), 7.05 (t, J = 7.4 Hz, 1H), 6.85 (s, 1H), 3.90–3.77 (m, 2H), 3.17–3.02 (m, 2H). ^{13} C NMR (100 MHz, DMSO-d_6): 159.9, 139.8, 136.7, 134.1, 127.5, 126.8, 125.0, 123.3, 121.5, 118.7, 118.6, 117.6, 111.9, 111.7, 111.2, 109.8, 42.8, 24.6. HRMS (ESI$^+$): m/z calcd for $C_{25}H_{20}ClN_7$, 454.1541, found, 454.1545.

*5.1.13. N^4-(2-(1H-indol-3-yl)ethyl)-6-bromo-N^2-(1H-indazol-5-yl) quinazoline-2,4-diamine (**9f**)*

Following the general procedure mentioned above, using **5f** (0.28 g, 1 mmol) as the starting material, compound **9f** was obtained as a light yellow solid (245 mg, 49%, two steps). Mp: decomp. above 283 °C. Rf: 0.23 (DCM/MeOH, 10/1, v/v). ^{1}H NMR (400 MHz, DMSO-d_6): 13.23 (s, 1H), 12.80 (br, 1H), 10.93 (s, 1H), 10.59 (s, 1H), 10.03 (s, 1H), 8.68 (s, 1H), 7.96–7.94 (m, 3H), 7.56 (d, J = 8.3 Hz, 1H), 7.51 (d, J = 8.8 Hz, 1H), 7.43 (d, J = 8.1 Hz, 2H), 7.35 (d, J = 8.1 Hz, 1H), 7.16 (s, 1H), 7.05 (t, J = 7.3 Hz, 1H), 6.87–6.84 (m, 1H), 3.84–3.83 (m, 2H), 3.11–3.07 (m, 2H). ^{13} C NMR (100 MHz, DMSO-d_6): 159.4, 152.7, 139.0, 138.3, 138.0, 136.7, 134.0, 129.7, 127.5, 127.1, 123.3, 121.5, 120.2, 118.8, 118.7, 116.6, 114.4, 112.5, 111.9, 111.7, 111.1, 42.9, 24.5. HRMS (ESI$^+$): m/z calcd for $C_{25}H_{20}BrN_7$, 500.1016, found, 500.1023.

*5.1.14. N^4-(2-(1H-indol-3-yl)ethyl)-6-fluoro-N^2-(1H-indazol-5-yl) quinazoline-2,4-diamine (**9g**)*

Following the general procedure mentioned above, using **5g** (0.22 g, 1 mmol) as the starting material, compound **9g** was obtained as a light yellow solid (140 mg, 32%, two steps). Mp: 264–267 °C. Rf: 0.20 (DCM/MeOH, 10/1, v/v). ^{1}H NMR (400 MHz, DMSO-d_6): 13.19 (s, 1H), 12.52 (br, 1H), 10.92 (s, 1H), 10.38 (s, 1H), 9.88 (s, 1H), 8.33 (d, J = 8.1 Hz, 1H), 7.99 (s, 1H), 7.92 (s, 1H), 7.73–7.70 (m, 1H), 7.63–7.59 (m, 1H), 7.55 (d, J = 8.7 Hz, 1H), 7.44 (d, J = 8.1 Hz, 2H), 7.35 (d, J = 8.1 Hz, 1H), 7.16 (s, 1H), 7.04 (t, J = 7.4 Hz, 1H), 6.85 (t, J = 7.2 Hz, 1H), 3.85–3.84 (m, 2H), 3.11–3.08 (m, 2H). ^{13} C NMR (100 MHz, DMSO-d_6): 160.0, 159.7, 157.3, 153.1, 138.4, 136.7, 133.9, 130.1, 127.5, 123.9, 123.6, 123.4, 123.3, 121.5, 121.0, 118.7, 118.7, 114.5, 111.9, 111.7, 111.1, 110.2, 110.0, 42.8, 24.6. HRMS (ESI$^+$): m/z calcd for $C_{25}H_{20}FN_7$, 438.1837, found, 438.1842.

*5.1.15. Sodium nitromalonaldehyde monohydrate (**11**)*

To a solution of $NaNO_2$ (20.0 g, 0.29 mol) in water (20 mL) was dropwise added a solution of mucobromic acid (20.0 g, 0.078 mol) in ethanol at 54 °C over 45 min, and the mixture was stirred at the same temperature for 15 min. The reaction was cooled to 0 °C and the solid was filtered to give sodium nitromalonaldehyde monohydrate (**11**) as an off-white solid (3.33 g, 27%). MS (ESI$^-$) m/z:115.4 [M−H]$^-$.

*5.1.16. 5-Nitro-1H-pyrazolo[3,4-b]pyridine (**12**)*

To a solution of sodium nitromalonaldehyde monohydrate (1.23 g, 7.81 mmol) in water was added 1*H*-pyrazol-3-amine (0.84 g, 7.43 mmol). The mixture was stirred at 90 °C for 16 h and then cooled to room temperature. The reaction solution was adjusted to pH = 5 and extracted by ethyl acetate (200 mL). The organic layer was dried over Na_2SO_4 and evaporated. The residue was purified by silica gel chromatography (1% MeOH in dichloromethane) to give 5-nitro-1*H*-pyrazolo [4,3-*b*]pyridine as a white solid (118 mg, 27%). Rf: 0.23 (DCM/MeOH, 100/1, v/v). Mp: 206–208 °C. ^{1}H NMR (DMSO-d_6, 400 MHz) δ 14.40 (s, 1H), 9.35 (d, J = 2.5 Hz, 1H), 9.21 (d, J = 2.5 Hz, 1H), 8.46 (s, 1H). MS (ESI$^-$) m/z:162.8 [M−H]$^-$.

*5.1.17. 1H-Pyrazolo[3,4-b]pyridin-5-amine (**13**)*

To a solution of 5-nitro-1*H*-pyrazolo [4,3-*b*]pyridine (7.3 g, 38.0 mmol) in MeOH (240 mL) was added 10% wt Pd/C (4.03, 3.8 mmol). The reaction mixture was hydrogenated under hydrogen (1 atm) for 16 h. The Pd/C was removed by filtration, and the filtrate was concentrated to give 1*H*-pyrazolo [4,3-*b*]pyridin-5-amine (5.1 g, 82% yield) as a light brown solid. Rf: 0.33 (DCM/MeOH, 19/1, v/v). Mp: 178 °C. ^{1}H NMR (DMSO-d_6, 400 MHz) δ 13.12 (s, 1H), 8.05 (d, J = 2.4 Hz, 1H), 7.81 (s, 1H), 7.18 (d, J = 2.3 Hz, 1H), 5.04 (s, 2H). MS (ESI$^+$) m/z:134.8 [M+H]$^+$, 156.7 [M+Na]$^+$, 301.0 [2M+Na]$^+$.

*5.1.18. 2-Chloro-6-methyl-4-nitroaniline (**15a**)*

To a solution of 2-methyl-4-nitroaniline (2.0 g, 13.2 mmol) in acetonitrile (40 mL) was added *N*-chlorosuccinimide (2.1 g, 15.8 mmol) at 60 °C. The mixture was heated to reflux for 3 h and then cooled to room temperature. The mixture was evaporated and diluted with dichloromethane (50 mL). The organic layer was washed with 2.5 M NaOH and brine, dried over Na_2SO_4, filtered, and evaporated. The residue was purified by silica gel chromatography (*n*-hexane/ethyl acetate, 4/1, v/v) to give 2-chloro-6-methyl-4-nitroaniline as a yellow solid (2.33 g, 95%). Mp: 172–174 °C. Rf: 0.40 (*n*-hexane/ethyl acetate, 5/1, v/v). ^{1}H NMR (DMSO-d_6, 400 MHz) δ 8.01 (d, J = 2.6 Hz, 1H), 7.89 (d, J = 2.1 Hz, 1H), 6.61 (s, 2H), 2.22 (s, 3H). MS (ESI$^-$) m/z:184.5 [M−H]$^-$.

*5.1.19. 2-Bromo-6-methyl-4-nitroaniline **(15b)***

To a solution of 2-methyl-4-nitroaniline (2.0 g, 13.2 mmol) in acetonitrile (40 mL) was added *N*-bromosuccinimide (2.8 g, 15.8 mmol) at 60 °C. The mixture was heated to reflux for 3 h and then cooled to room temperature. The mixture was evaporated and diluted with dichloromethane (50 mL). The organic layer was washed with 2.5 M NaOH and brine, dried over Na_2SO_4, filtered, and evaporated. The residue was purified by silica gel chromatography (*n*-hexane/ethyl acetate, 4/1, v/v) to give 2-bromo-6-methyl-4-nitroaniline as a yellow solid (2.75 g, 91%). Mp: 178–179 °C. Rf: 0.40 (*n*-hexane/ethyl acetate, 5/1, v/v). ^{1}H NMR (DMSO-d_6, 400 MHz) δ 8.15 (d, J = 2.5 Hz, 1H), 7.93 (d, J = 2.1 Hz, 1H), 6.53 (s, 2H), 2.23 (s, 3H). MS (ESI$^-$) m/z:228.5 [M−H]$^-$.

*5.1.20. 7-Chloro-5-nitro-1H-indazole (**16a**)*

To a 0 °C solution of 2-chloro-6-methyl-4-nitroaniline (**15a**) (0.9 g, 4.9 mmol) in glacial acetic acid (18 mL) was added a solution of $NaNO_2$ (0.40 g, 5.8 mmol) in 4 mL water dropwise over a period of 10 min with stirring. The mixture was allowed to warm to room temperature and stirred for 12 h. The precipitate was removed by filtration of the reaction mixture through a pad of Celite. The filtrate was poured into H_2O (100 mL); the solid was collected by filtration and purified by silica gel column chromatography (DCM/MeOH 100:1 as eluent) to afford **16a** as a light brown solid (0.50 g, 52%). Mp: 250–251 °C. Rf: 0.47 (DCM/MeOH, 100/1, v/v). ^{1}H NMR (DMSO-d_6, 400 MHz) δ 14.33 (s, 1H), 8.86 (d, J = 1.3 Hz, 1H), 8.53 (s, 1H), 8.30 (s, 1H). MS (ESI$^-$) m/z:195.5 [M - H]$^-$.

*5.1.21. 7-Bromo-5-nitro-1H-indazole (**16b**)*

Compound **16b** was prepared in a manner similar to that of **16a** as a light brown solid (49%). Rf: 0.53 (DCM/MeOH, 100/1, v/v). Mp: 250–251 °C. ^{1}H NMR (DMSO-d_6, 400 MHz) δ 14.22 (s, 1H), 8.88 (d, J = 1.2 Hz, 1H), 8.55 (s, 1H), 8.42 (d, J = 1.7 Hz, 1H). MS (ESI$^-$) m/z:239.5 [M - H]$^-$.

*5.1.22. 7-Chloro-1H-indazol-5-amine (**17a**)*

A mixture of 7-chloro-5-nitro-1*H*-indazole (**16a**) (200 mg, 0.94 mmol), $SnCl_2$-H_2O (1.0 g, 4.7 mmol) in EtOH (10 mL) was heated at reflux for 18 h. After filtration, the filtrate was concentrated to yield 164 mg (97%) of 1H-indazol-5-amine as a light brown solid. Rf: 0.25 (DCM/MeOH, 100/1, v/v). Mp: 157–159 °C. ^{1}H NMR (DMSO-d_6, 400 MHz) δ 13.02 (s, 1H), 7.84 (d, J = 1.0 Hz, 1H), 6.88 (d, J = 1.6 Hz, 1H), 6.73 (s, 1H), 4.99 (s, 2H). MS (ESI$^+$) m/z:167.7 [M+H]$^+$.

*5.1.23. 7- Bromo-1H-indazol-5-amine (**17b**)*

Compound **17b** was prepared in a manner similar to that for **17a** as a light brown solid (92%). Rf: 0.23 (DCM/MeOH, 100/1, v/v). Mp: 165–167 °C. ^{1}H NMR (DMSO-d_6, 400 MHz) δ 12.93 (s, 1H), 7.86 (d, J = 8.1 Hz, 1H), 7.02 (d, J = 1.6 Hz, 1H). MS (ESI) m/z: 211.7[M+H]$^+$.

*5.1.24. N-(2, 6-dimethylphenyl)-4-methylbenzenesulfonamide (**19**)*

A mixture of 2, 6-dimethylaniline (2.4 g, 20 mmol), 4-toluenesulfonyl chloride (2.5 g, 13.2 mmol) and silica gel (14.4 g, 100–200 mesh) was stirred at room temperature. The progress of the reaction was monitored by TLC. After completion of the reaction, MeOH (100 mL) was added, and the mixture was filtered through a sintered funnel. The solvent was evaporated and the residue was purified by recrystallization (MeOH) to give the product **19** as a white solid (4.79 g, 87%). Rf: 0.57 (*n*-hexane/ethyl acetate, 5/1, v/v). Mp: 134–135 °C. ^{1}H NMR ($CDCl_3$, 400 MHz) δ 7.61 (d, J = 8.3 Hz, 2H), 7.26 (d, J = 8.5 Hz, 2H), 7.12–7.09 (m, 1H), 7.04 (s, 1H), 7.02 (s, 1H), 6.57 (s, 1H), 2.44 (s, 3H), 2.05 (s, 6H). MS (ESI$^+$) m/z: 275.9 [M+H]$^+$, 298.0 [M+Na]$^+$.

*5.1.25. N-(2,6-dimethyl-4-nitrophenyl)-4-methylbenzenesulfonamide **(20)***

N-tosyl-2-6-dimethylaniline (**19**) (2.0 g, 7.3 mmol) was suspended in 100 mL AcOH-H_2O-HNO_3 (1:1:0.2) mixture. Sodium nitrite (1.0 g, 14.6 mmol) was added and the reaction mixture was reflux for 4 h. The reaction was monitored via TLC and, upon completion, was allowed to cool to room temperature overnight to yield colourless crystals. The crystals were filtered and washed with water to afford 1.6 g (70%) of **20**. Rf: 0.73 (DCM). Mp: 163–164 °C. ^{1}H NMR ($CDCl_3$, 400 MHz) 7.92 (s, 2H), 7.61 (d, J = 8.2 Hz, 2H), 7.31 (s, 1H), 7.29 (s, 1H), 6.02 (s, 1H), 2.46 (s, 3H), 2.17 (s, 6H). MS (ESI$^-$) m/z: 318.7 [M - H]$^-$.

*5.1.26. 2,6-dimethyl-4-nitroaniline (**21**)*

N-Tosyl-2,6-dimethyl-4-nitroaniline (**20**) (3.2 g, 10.0 mmol) was dissolved in H_2SO_4 (32 mL) and warmed at 50 °C for 1 h. The reaction mixture was poured slowly into an ice/water mixture. The precipitate was filtered and washed with water. The crude product was purified by recrystallization (ethyl acetate) to give **21** as yellow crystals (1.0 g, 53%). Rf: 0.34 (*n*-hexane/ethyl acetate, 5/1, v/v). Mp: 164–165 °C. ^{1}H NMR (DMSO-d_6, 400 MHz) δ 7.79 (s, 2H), 6.16 (s, 2H), 2.16 (s, 6H). MS (ESI$^+$) m/z: 166.8 [M+H]$^+$, 188.8 [M+Na]$^+$.

*5.1.27. 7-methyl-5-nitro-1H-indazole (**22**)*

To a 0 °C solution of 2,6-dimethyl-4-nitroaniline (**21**) (0.9 g, 5.4 mmol) in glacial acetic acid (18 mL) was added a solution of $NaNO_2$ (0.45 g, 6.5 mmol) in 5 mL water by dropwise addition over a period of 10 min with stirring. The mixture was allowed to warm to room temperature and stirred for 12 h. The precipitate was removed by filtration of the reaction mixture through a pad of Celite. The filtrate was poured into H_2O (100 ml); the solid was collected by filtration and purified by silica gel column chromatography (DCM/MeOH 100:1 as eluent) to afford **22** as a yellow solid (0.50 g, 52%). Mp: 247–248 °C. Rf: 0.24 (DCM/MeOH, 100/1, v/v). ^{1}H NMR (DMSO-d_6, 400 MHz) δ 13.83 (s, 1H), 8.67 (d, J = 1.8 Hz, 1H), 8.39 (d, J = 1.1 Hz, 1H), 8.02 (s, 2H), 2.62 (s, 3H). MS (ESI$^-$) m/z: 175.5 [M–H]$^-$.

*5.1.28. 7-Methyl-1H-indazol-5-amine (**23**)*

A mixture of 7-methyl-5-nitro-1*H*-indazole (**22**) (0.23 g, 1.3 mmol) and 10% Pd/C (50 mg) in MeOH (4 mL) was stirred under H_2 (1 atm) overnight. After filtration, the filtrate was concentrated to yield 7-methyl-1*H*-indazol-5-amine (**23**) as a brown solid without further purification (188 mg, 97%). Rf: 0.40 (DCM/MeOH, 19/1, v/v). Mp: 134–136 °C. ^{1}H NMR (DMSO-d_6, 400 MHz) δ 12.64 (s, 1H), 7.69 (s, 1H), 6.55 (s, 2H), 4.66 (s, 2H), 2.38 (s, 3H). MS (ESI$^+$) m/z: 147.8 [M+H]$^+$.

Compounds **24a-h** were synthesized by the same procedure as described for synthesis of compound **9a**.

*5.1.29. N^4-(2-(1H-indol-3-yl)ethyl)-N^2-(1H-benzo[d] [1-3]triazol-5-yl)-6-chloroquinazoline-2,4-diamine (**24a**)*

Using **8d** (179 mg, 0.5 mmol) and 1*H*-benzo[d] [1-3]triazol-5-amine (67 mg, 0.5 mmol) as starting materials, compound **24a** was prepared as an off-white solid (168 mg, 74%). Mp: 218–219 °C. Rf: 0.31 (DCM/MeOH, 10/1, v/v). ^{1}H NMR (400 MHz, DMSO-d_6): δ ppm 13.03 (br, 1H), 10.86 (s, 1H), 10.74 (s, 1H), 10.07 (s, 1H), 9.92 (s, 1H), 8.57 (d, J = 1.1 Hz, 1H), 7.90 (dd, J = 1.3, 5.9 Hz, 1H), 7.75–7.65 (m, 3H), 7.42 (t, J = 5.2 Hz, 1H), 7.32 (d, J = 5.4 Hz, 2H), 7.04 (t, J = 5.0 Hz, 1H), 6.91 (t, J = 4.9 Hz, 1H), 6.82 (d, J = 5.1 Hz, 1H), 3.76 (s, 2H), 2.95 (s, 2H). ^{13}C NMR (100 MHz, DMSO-d_6): 159.7, 152.0, 138.1, 136.7, 135.7, 129.4, 127.4, 124.4, 123.2, 121.4, 120.0, 118.8, 118.6, 112.2, 111.9, 111.4, 43.0, 24.6. HRMS (ESI$^+$): m/z calcd for $C_{24}H_{19}ClN_8$, 455.1498, found, 455.1494.

*5.1.30. N^4-(2-(1H-indol-3-yl)ethyl)-N^2-(1H-benzo[d]imidazol-5-yl)-6-chloroquinazoline-2,4-diamine (**24b**)*

Using **8d** (179 mg, 0.5 mmol) and 1*H*-benzo[*d*]imidazol-5-amine (67 mg, 0.5 mmol) as starting materials, compound **24b** was prepared as an off-white solid (186 mg, 82%). Mp: decomp. above 214 °C. Rf: 0.07 (DCM/MeOH, 10/1, v/v). ^{1}H NMR (400 MHz, DMSO-d_6): δ ppm 10.87 (s, 1H), 10.43 (s, 1H), 9.60 (s, 1H), 8.99 (s, 1H), 8.49 (s, 1H), 8.21 (s, 1H), 7.81 (d, J = 8.2 Hz, 2H), 7.70 (d, J = 8.7 Hz, 1H), 7.59–7.56 (m, 2H), 7.44 (d, J = 7.2 Hz, 1H), 7.33 (d, J = 7.9 Hz, 1H), 7.18 (s, 1H), 7.04 (t, J = 7.0 Hz, 1H), 6.84 (t, J = 7.0 Hz, 1H), 3.87–3.86 (m, 2H), 3.13–3.11 (m, 2H). ^{13}C NMR (100 MHz, DMSO-d_6): 159.7, 153.9, 141.8, 136.7, 134.9, 128.7, 128.1, 127.6, 123.8, 123.4, 122.2, 121.4, 119.7, 118.6, 115.5, 112.4, 111.9, 107.7, 42.8, 24.6. HRMS (ESI$^+$): m/z

calcd for $C_{25}H_{19}ClN_7$, 454.1541, found, 454.1536.

*5.1.31. 5-((4-((2-(1H-indol-3-yl)ethyl)amino)-6-chloroquinazolin-2-yl)amino)indolin-2-one (**24c**)*

Using **8d** (179 mg, 0.5 mmol) and 5-aminoindolin-2-one (74 mg, 0.5 mmol) as starting materials, compound **24c** was prepared as an off-white solid (180 mg, 77%). Mp: decomp. above 212 °C. Rf: 0.34 (DCM/MeOH, 10/1, v/v). ^{1}H NMR (600 MHz, DMSO-d_6): δ ppm 12.65 (br, 1H), 10.90 (s, 1H), 10.46 (s, 1H), 10.38 (s, 1H), 9.92 (s, 1H), 8.51 (d, J = 2.0 Hz, 1H), 7.84 (dd, J = 1.8, 8.9 Hz, 1H), 7.58 (d, J = 8.8 Hz, 1H), 7.43 (s, 1H), 7.40 (s, 1H), 7.34 (d, J = 8.1 Hz, 1H), 7.27 (d, J = 8.1 Hz, 1H), 7.18 (s, 1H), 7.05 (t, J = 7.4 Hz, 1H), 6.90 (t, J = 7.3 Hz, 1H), 6.82 (d, J = 7.7 Hz, 1H),3.82−3.81 (m, 2H), 3.09−3.07 (m, 2H). ^{13}C NMR (100 MHz, DMSO-d_6): 159.4, 152.0, 138.0, 136.7, 135.5, 128.9, 127.5, 126.9, 124.3, 123.3, 121.5, 119.6, 118.7, 118.6, 111.9, 111.9, 111.7, 109.7, 43.0, 36.3, 24.5. HRMS (ESI$^+$): m/z calcd for $C_{26}H_{20}ClN_6O$, 469.1538, found, 469.1538.

*5.1.32. N^4-(2-(1H-indol-3-yl)ethyl)-6-chloro-N^2-(1H-indazol-6-yl) quinazoline-2,4-diamine (**24d**)*

Using **8d** (179 mg, 0.5 mmol) and 1*H*-indazol-6-amine (67 mg, 0.5 mmol) as starting materials, compound **24d** was prepared as an off-white solid (152 mg, 76%). Mp: decomp. above 217 °C. Rf: 0.42 (DCM/MeOH, 10/1, v/v). ^{1}H NMR (400 MHz, DMSO-d_6): δ ppm 13.17 (s, 1H), 12.72 (br, 1H), 10.86 (s, 1H), 10.70 (s, 1H), 9.97 (s, 1H), 8.54 (d, J = 2.0 Hz, 1H), 8.08 (s, 1H), 7.88−7.85 (m, 2H), 7.76 (d, J = 8.6 Hz, 2H), 7.61 (d, J = 8.9 Hz, 1H), 7.46 (d, J = 7.9 Hz, 1H), 7.33 (d, J = 8.1 Hz, 1H), 7.26 (dd, J = 1.3, 8.6 Hz, 1H), 7.14 (d, J = 1.4 Hz, 1H), 7.03 (t, J = 7.4 Hz, 1H), 6.84 (t, J = 7.5 Hz, 1H), 3.91−3.86 (m, 2H), 3.15−3.11 (m, 2H). ^{13}C NMR (100 MHz, DMSO-d_6): 159.7, 152.2, 140.7, 138.1, 136.7, 135.6, 135.1, 133.9, 129.1, 127.6, 124.3, 123.5, 121.5, 121.4, 120.9, 119.9, 118.7, 117.1, 112.1, 112.1, 111.9, 111.6, 103.5, 43.2, 24.4. HRMS (ESI$^+$): m/z calcd for $C_{25}H_{19}ClN_7$, 454.1541, found, 454.1547.

*5.1.33. N^4-(2-(1H-indol-3-yl)ethyl)-6-chloro-N^2-(1H-pyrazolo [3,4-b]pyridin-5-yl)quinazoline-2,4-diamine (**24e**)*

Using **8d** (179 mg, 0.5 mmol) and 1*H*-pyrazolo [3,4-*b*]pyridin-5-amine (**13**, 67 mg, 0.5 mmol) as starting materials, compound **24e** was prepared as an off-white solid (134 mg, 59%). Mp: decomp. above 278 °C. Rf: 0.37 (DCM/MeOH, 10/1, v/v). ^{1}H NMR (400 MHz, DMSO-d_6): δ ppm 13.81 (s, 1H), 10.90 (s, 1H), 10.57 (s, 1H), 9.99 (s, 1H), 8.64 (d, J = 2.2 Hz, 1H), 8.55 (s, 1H), 8.38 (s, 1H), 8.04 (s, 1H), 7.87 (d, J = 8.0 Hz, 1H), 7.64 (d, J = 8.9 Hz, 1H), 7.39 (s, 1H), 7.34 (d, J = 8.1 Hz, 1H), 7.13 (s, 1H), 7.04 (t, J = 7.2 Hz, 1H), 6.83 (s, 1H), 3.77 (s, 2H), 3.05 (s, 2H). ^{13}C NMR (100 MHz, DMSO-d_6): 159.6, 153.2, 146.4, 136.7, 135.4, 133.7, 128.9, 127.5, 124.4, 123.3, 121.4, 118.7, 118.6, 114.6, 112.3, 111.9, 111.6, 42.8, 24.6. HRMS (ESI$^+$): m/z calcd for $C_{24}H_{19}ClN_8$, 455.1498, found, 455.1505.

*5.1.34. N^4-(2-(1H-indol-3-yl)ethyl)-6-chloro-N^2-(7-chloro-1H-indazol-5-yl)quinazoline-2,4-diamine (**24f**)*

Using **8d** (179 mg, 0.5 mmol) and **17a** (84 mg, 0.5 mmol) as starting materials, compound **24f** was prepared as an off-white solid (124 mg, 51%). Mp: decomp. above 297 °C. Rf: 0.42 (DCM/MeOH, 10/1, v/v). ^{1}H NMR (400 MHz, DMSO-d_6): δ ppm13.71 (s, 1H), 12.54 (br, 1H), 10.89 (s, 1H), 10.55 (s, 1H), 9.89 (s, 1H), 8.50 (d, J = 1.6 Hz, 1H), 8.12 (s, 1H), 7.90 (s, 1H), 7.86 (d, J = 9.0 Hz, 2H), 7.70 (s, 1H), 7.62 (d, J = 8.9 Hz, 1H), 7.40 (s, 1H), 7.34 (d, J = 8.2 Hz, 1H), 7.16 (s, 1H), 7.04 (t, J = 7.5 Hz, 1H), 6.82 (s, 1H), 3.82−3.81 (m, 2H), 3.10−3.07 (m, 2H). ^{13}C NMR (100 MHz, DMSO-d_6): 159.6, 152.9, 136.7, 136.1, 135.4, 130.8, 128.8, 127.5, 124.8, 124.2, 123.3, 122.9, 121.4, 120.4, 118.7, 118.7, 115.4, 112.2, 111.9, 111.7, 42.9, 24.5. HRMS (ESI$^+$): m/z calcd for $C_{25}H_{19}Cl2N_7$, 488.1152, found, 488.1150.

*5.1.35. N^4-(2-(1H-indol-3-yl)ethyl)-N^2-(7-bromo-1H-indazol-5-yl)-6-chloroquinazoline-2,4-diamine (**24g**)*

Using **8d** (179 mg, 0.5 mmol) and **17b** (106 mg, 0.5 mmol) as starting materials, compound **24g** was prepared as an off-white solid (125 mg, 47%). Mp: decomp. above 289 °C. Rf: 0.42 (DCM/MeOH, 10/1, v/v). ^{1}H NMR (400 MHz, DMSO-d_6): δ ppm 13.62 (s, 1H), 10.90 (s, 1H), 10.61 (s, 1H), 9.96 (s, 1H), 8.53 (d, J = 1.8 Hz, 1H), 8.13 (s, 1H), 7.94 (s, 1H), 7.87−7.85 (m, 2H), 7.62 (d, J = 8.9 Hz, 1H), 7.39 (s, 1H), 7.34 (d, J = 8.1 Hz, 1H), 7.17 (s, 1H), 7.04 (t, J = 7.4 Hz, 1H), 6.82 (s, 1H), 3.83−3.81 (m, 2H), 3.11−3.08 (m, 2H). ^{13}C NMR (100 MHz, DMSO-d_6): 159.6, 152.6, 136.7, 135.4, 130.8, 128.9, 127.5, 125.9, 124.2, 123.3, 121.4, 120.1, 118.7, 118.6, 112.1, 111.9, 111.6, 43.0, 24.5. HRMS (ESI$^+$): m/z calcd for $C_{25}H_{19}BrClN_7$, 534.0626, found, 534.0630.

*5.1.36. N^4-(2-(1H-indol-3-yl)ethyl)-6-chloro-N^2-(7-methyl-1H-indazol-5-yl)quinazoline-2,4-diamine (**24h**)*

Using **8d** (179 mg, 0.5 mmol) and **23** (74 mg, 0.5 mmol) as starting materials, compound **24h** was prepared as an off-white solid (150 mg, 64%). Mp: decomp. above 289 °C. Rf: 0.40 (DCM/MeOH, 10/1, v/v). ^{1}H NMR (100 MHz, DMSO-d_6): δ ppm 13.29 (s, 1H), 10.93 (s, 1H), 10.52 (s, 1H), 9.96 (s, 1H), 8.53 (d, J = 2.0 Hz, 1H), 7.94 (s, 1H), 7.85 (d, J = 8.6 Hz, 1H), 7.76 (s, 1H), 7.59 (d, J = 8.9 Hz, 1H), 7.43 (s, 1H), 7.35 (d, J = 8.1 Hz, 1H), 7.25 (s, 1H), 7.17 (s, 1H), 7.05 (t, J = 7.3 Hz, 1H), 6.84 (s, 1H), 3.85−3.84 (m, 2H), 3.12−3.09 (m, 2H), 2.45 (s, 3H). ^{13}C NMR (100 MHz, DMSO-d_6): 159.5, 152.4, 138.6, 138.2, 136.7, 135.4, 134.3, 128.8, 127.5, 124.3, 123.2, 123.0, 121.5, 121.2, 119.7, 118.7, 118.6, 111.9, 111.7, 42.9, 24.5, 17.3. HRMS (ESI$^+$): m/z calcd for $C_{26}H_{21}ClN_7$, 468.1698, found, 468.1695.

5.2. Pharmacological assay

5.2.1. PAK4 HTRF assays

The PAK4 kinase assay was performed using HTRF® KinEASE™-STK kit (Cisbio Bioassays, France) in 384-well low volume microplate (Nunc, ThermoFisher Scientific). Purified enzyme of PAK4 was purchased from Carna Biosciences (Japan) The kinase activity was assessed under conditions determined experimentally. Specifically, PAK4 0.0256 ng/uL was incubated with saturating concentration of substrate S2 at 1 μM and Km concentration of ATP at 4 μM, with or without compounds in 5 mM $MgCl_2$, 1 mM DTT and 1X KinEASE enzymatic buffer at a total volume of 10 μL. The enzymatic reaction was started by adding kinase, incubated at R.T. for 40 min, and terminated by adding 10 μL EDTA-containing detection reagents, prepared according to kit instruction. Kinase activity was at the linear range with protein amount and incubation time. HTRF signal was obtained by reading the plate in Infinite® F500 microplate reader (Tecan, Switzerland). Test compounds were prepared in DMSO at stock solutions of 20 mM. For primary compound screening, compounds were diluted in kinase reaction buffer and tested at 100, 10 and 1.0 μM in 10 μL kinase reaction with DMSO below or at 0.5%. For IC_{50} studies, compounds were 5X serial diluted from 1000 μM to 0.1 nM using kinase reaction buffer. IC_{50}s were obtained by fitting data to sigmoidal dose-response curve.

5.2.2. Anti-proliferative assay

The human pulmonary carcinoma cell line A-549 was cultured in RPMI-1640 medium containing 10% FBS, 100 U/mL streptomycin and 100 U/mL penicillin at 37 °C in a humidified atmosphere containing 5% CO_2.

A549 cells (1×10^4/well) were plated in 0.1 mL of a medium containing 10% FBS in 96-well Corning plates. After 24 h, the medium was removed and replaced with 0.1 mL medium containing the indicated concentrations of the compound **9d** for 24, 48, or 72 h. At the end of the incubation, the cellular proliferation was

measured by the modified tetrazolium salt 3-(4, 5-dimethylthiozol-2-yl)-2, 5-biphenyl-tetrazolium bromide (MTT, Sigma) assay. For this, 0.01 mL MTT solution (5 mg/mL in PBS) was added to each well. After 4 h incubation at 37 °C, the medium was replaced by 0.15 mL DMSO. After 15 min incubation at 37 °C, the optical densities at 490 nm were measured using a Microplate Reader (BIO-RAD). The data were calculated and plotted as the percent viability compared to the control. The 50% inhibitory concentration (IC_{50}) was defined as the concentration that reduced the absorbance of the untreated wells by 50% of the vehicle in the MTT assay.

5.2.3. Cell-cycle analysis by flow cytometry

A549 cells (8×10^4 cells) were incubated with the indicated concentrations of **9d** for 24 h. After incubation, cells were collected, washed with PBS, and suspended in a staining buffer (10 μg/mL propidium iodide, 0.5% Tween-20, 0.1% RNase in PBS). The cells were analysed using a FACSVantage flow cytometer with the Cell Quest acquisition and analysis software program (Becton Dickinson and Co., San Jose, CA).

5.2.4. Western blot assay

To determine the expression of protein, whole cell extracts were prepared from 1×10^6 cells in RIPA lysis buffer (50 mM Tris/HCl pH 7.4, 150 mM NaCl, 1% Nonidet P-40, 0.25% Na-deoxycholate, 1 mM EDTA and protease inhibitor cocktail). Equal amounts of denatured protein were separated by SDS-PAGE and transferred to a PVDF membrane (Millipore). The membrane was blocked with 5% nonfat dry milk in TBS-T (20 mM Tris, pH 7.4, 137 mM NaCl, 0.05% Tween-20) for 3 h at room temperature, and the proteins were probed with antibodies specific to CDK2, CDK4, CDK6, cyclinD1, cyclinD3, $p18^{ink4c}$, $p21^{Cip1/Waf1}$, $p27^{Kip1}$, LIMK1, phospho-LIMK1, PAK4, and phospho-PAK4/Ser474. All PVDF membranes were detected by chemiluminescence (ECL, Pierce Technology). To assure equal loading, membranes were stripped and reprobed with antibodies against GAPDH and MMP2 (Shang Hai Kangchen).

5.2.5. Cell migration and invasion assays

Migration and invasion assays were performed using modified Boyden chambers with a polycarbonate nucleopore membrane. Pre-coated filters (6.5 mm in diameter, 8 μm pore size and Matrigel 100 $\mu g/cm^2$) for the invasion assay were rehydrated with 100 μL medium. Then, 1×10^5 cells in 100 μL serum-free DMEM supplemented with 0.1% bovine serum were placed in the upper part of each chamber and the lower compartments were filled with 600 μL DMEM containing 10% serum. After incubation for 12 h at 37 °C, the non-invaded or non-migrated cells were removed from the upper surface of the filter with a cotton swab, and the invaded/migrated cells on the lower surface of the filter were fixed, stained, photographed, and counted under high-power magnification.

5.2.6. Statistical analysis

All statistical analyses were carried out using SPSS 16.0 software, and the results were considered statistically significant at a *P*-value <0.05.

5.3. Molecular docking study

Ensemble docking was performed with AutoDock 4 into the predefined kinase ATP-binding pocket [29]. Hydrogens were added to the modelled PAK4 kinase domain (PDB code 4NJD), and partial atomic charges were assigned using AutoDockTools (ADT). The ligand coordinates were generated using the Corina server (https://www.mn-am.com/online_demos/corina_demo). The ligand was placed in the kinase ATP-binding pocket and aligned manually to avoid atom clashes. A 3D grid box (dimensions = 50 × 50 × 50 units in number of grid points; grid spacing = 0.375 Å) centred at the ATP-binding pocket was created using AutoGrid4. Docking was performed using the Lamarckian genetic algorithm in AutoDock4. Each docking experiment was performed 10 times, yielding 10 docked conformations. The solutions were ranked by the calculated binding free energy. Figures were drawn using PyMOL.

Acknowledgments

We gratefully acknowledge the financial support from the National Natural Science Foundation of China (Grant 81230077) and Program for Innovative Research Team of the Ministry of Education, and Program for Liaoning Innovative Research Team in University.

Appendix A. Supplementary data

Supplementary data associated with this article can be found in the online version, at http://dx.doi.org/10.1016/j.ejmech.2017.02.063. These data include MOL files and InChiKeys of the most important compounds described in this article.

References

[1] M. Radu, G. Semenova, R. Kosoff, J. Chernoff, PAK signalling during the development and progression of cancer, Nat. Rev. Cancer 14 (2014) 13–25.
[2] L.E. Arias-Romero, J. Chernoff, A tale of two PAKs, Biol. Cell 100 (2008) 97–108.
[3] M.G. Callow, F. Clairvoyant, S. Zhu, B. Schryver, D.B. Whyte, J.R. Bischoff, B. Jallal, T. Smeal, Requirement for PAK4 in the anchorage-independent growth of human cancer cell lines, J. Biol. Chem. 277 (2002) 550–558.
[4] S. Chen, T. Auletta, O. Dovirak, C. Hutter, K. Kuntz, S. El-ftesi, J. Kendall, H. Han, D.D. Von Hoff, R. Ashfaq, A. Maitra, C.A. Iacobuzio-Donahue, R.H. Hruban, R. Lucito, Copy number alterations in pancreatic cancer identify recurrent PAK4 amplification, Cancer Biol. Ther. 7 (2008) 1793–1802.
[5] Y. Liu, H. Xiao, Y. Tian, T. Nekrasova, X. Hao, H.J. Lee, N. Suh, C.S. Yang, A. Minden, The pak4 protein kinase plays a key role in cell survival and tumorigenesis in athymic mice, Mol. Cancer Res. 6 (2008) 1215–1224.
[6] G.D. Hu, Y.H. Chen, L. Zhang, W.C. Tong, Y.X. Cheng, Y.L. Luo, S.X. Cai, L. Zhang, The generation of the endothelial specific cdc42-deficient mice and the effect of cdc42 deletion on the angiogenesis and embryonic development, Chin. Med. J. (Engl) 124 (2011) 4155–4159.
[7] F. Gnad, A. Young, W. Zhou, K. Lyle, C.C. Ong, M.P. Stokes, J.C. Silva, M. Belvin, L.S. Friedman, H. Koeppen, A. Minden, K.P. Hoeflich, Systems-wide analysis of K-Ras, Cdc42, and PAK4 signaling by quantitative phosphoproteomics, Mol. Cell Proteomics 12 (2013) 2070–2080.
[8] S.W. Cai, Z.Q. Ye, X.H. Wang, Y.H. Pan, Y.M. Weng, S. Lao, H.B. Wei, L. Li, Overexpression of P21-activated kinase 4 is associated with poor prognosis in non-small cell lung cancer and promotes migration and invasion, J. Exp. Clin. Cancer Res. 34 (2015).
[9] P.R. Molli, D.Q. Li, B.W. Murray, S.K. Rayala, R. Kumar, PAK signaling in oncogenesis, Oncogene 28 (2009) 2545–2555.
[10] C.M. Wells, G.E. Jones, The emerging importance of group II PAKs, Biochem. J. 425 (2010) 465–473.
[11] J. Rudolph, J.J. Crawford, K.P. Hoeflich, W. Wang, Inhibitors of p21-activated kinases (PAKs), J. Med. Chem. 58 (2015) 111–129.
[12] J.J. Crawford, K.P. Hoeflich, J. Rudolph, p21-Activated kinase inhibitors: a patent review, Expert Opin. Ther. Pat. 22 (2012) 293–310.
[13] B.W. Murray, C. Guo, J. Piraino, J.K. Westwick, C. Zhang, J. Lamerdin, E. Dagostino, D. Knighton, C.M. Loi, M. Zager, E. Kraynov, I. Popoff, J.G. Christensen, R. Martinez, S.E. Kephart, J. Marakovits, S. Karlicek, S. Bergqvist, T. Smeal, Small-molecule p21-activated kinase inhibitor PF-3758309 is a potent inhibitor of oncogenic signaling and tumor growth, Proc. Natl. Acad. Sci. U. S. A. 107 (2010) 9446–9451.
[14] T.M. Pitts, G.N. Kulikowski, A.C. Tan, B.W. Murray, J.J. Arcaroli, J.J. Tentler, A. Spreafico, H.M. Selby, M.I. Kachaeva, K.L. McPhillips, B.C. Britt, E.L. Bradshaw-Pierce, W.A. Messersmith, M. Varella-Garcia, S.G. Eckhardt, Association of the epithelial-to-mesenchymal transition phenotype with responsiveness to the p21-activated kinase inhibitor, PF-3758309, in colon cancer models, Front. Pharmacol. 4 (2013) 35.
[15] E.L. Bradshaw-Pierce, T.M. Pitts, A.C. Tan, K. McPhillips, M. West, D.L. Gustafson, C. Halsey, L. Nguyen, N.V. Lee, J.L. Kan, B.W. Murray, S.G. Eckhardt, Tumor P-Glycoprotein correlates with efficacy of PF-3758309 in in vitro and in vivo models of colorectal cancer, Front. Pharmacol. 4 (2013) 22.
[16] S.T. Staben, J.A. Feng, K. Lyle, M. Belvin, J. Boggs, J.D. Burch, C.C. Chua, H. Cui, A.G. DiPasquale, L.S. Friedman, C. Heise, H. Koeppen, A. Kotey, R. Mintzer, A. Oh, D.A. Roberts, L. Rouge, J. Rudolph, C. Tam, W. Wang, Y. Xiao, A. Young, Y. Zhang, K.P. Hoeflich, Back pocket flexibility provides group II p21-activated kinase (PAK) selectivity for type I 1/2 kinase inhibitors, J. Med. Chem. 57

(2014) 1033–1045.
[17] J.K. Park, S. Kim, Y.J. Han, S.H. Kim, N.S. Kang, H. Lee, S. Park, The discovery and the structural basis of an imidazo[4,5-b]pyridine-based p21-activated kinase 4 inhibitor, Bioorg Med. Chem. Lett. 26 (2016) 2580–2583.
[18] C.Z. Hao, X.D. Li, S. Song, B.Y. Guo, J. Guo, J. Zhang, Q.L. Zhang, W.X. Huang, J. Wang, B. Lin, M.S. Cheng, F. Li, D.M. Zhao, Advances in the 1-phenanthryl-tetrahydroisoquinoline series of PAK4 inhibitors: potent agents restrain tumor cell growth and invasion, Org. Biomol. Chem. 14 (2016) 7676–7690.
[19] O. Abu Aboud, C.H. Chen, W. Senapedis, E. Baloglu, C. Argueta, R.H. Weiss, Dual and Specific Inhibition of NAMPT and PAK4 By KPT-9274 decreases kidney cancer growth, Mol. Cancer Ther. 15 (2016) 2119–2129.
[20] J. Zhang, J. Wang, Q. Guo, Y. Wang, Y. Zhou, H. Peng, M. Cheng, D. Zhao, F. Li, LCH-7749944, a novel and potent p21-activated kinase 4 inhibitor, suppresses proliferation and invasion in human gastric cancer cells, Cancer Lett. 317 (2012) 24–32.
[21] B.J. Ryu, S. Kim, B. Min, K.Y. Kim, J.S. Lee, W.J. Park, H. Lee, S.H. Kim, S. Park, Discovery and the structural basis of a novel p21-activated kinase 4 inhibitor, Cancer Lett. 349 (2014) 45–50.
[22] S. Wenglowsky, L. Ren, K.A. Ahrendt, E.R. Laird, I. Aliagas, B. Alicke, A.J. Buckmelter, E.F. Choo, V. Dinkel, B.N.A. Feng, S.L. Gloor, S.E. Gould, S. Gross, J. Gunzner-Toste, J.D. Hansen, G. Hatzivassiliou, B.N. Liu, K. Malesky, S. Mathieu, B. Newhouse, N.J. Raddatz, Y.Q. Ran, S. Rana, N. Randolph, T. Risom, J. Rudolph, S. Savage, L.T. Selby, M. Shrag, K. Song, H.L. Sturgis, W.C. Voegtli, Z.Y. Wen, B.S. Willis, R.D. Woessner, W.I. Wu, W.B. Young, J. Grina, Pyrazolopyridine inhibitors of B-Raf(V600E). Part 1: the development of selective, orally bioavailable, and efficacious inhibitors, Acs Med. Chem. Lett. 2 (2011) 342–347.
[23] G. Wolber, T. Langer, LigandScout: 3-d pharmacophores derived from protein-bound Ligands and their use as virtual screening filters, J. Chem. Inf. Model 45 (2005) 160–169.
[24] B.Y. Guo, X.D. Li, S. Song, M. Chen, M.S. Cheng, D.M. Zhao, F. Li, (-)-Beta-hydrastine suppresses the proliferation and invasion of human lung adenocarcinoma cells by inhibiting PAK4 kinase activity, Oncol. Rep. 35 (2016) 2246–2256.
[25] J. Marshall, Transwell((R)) invasion assays, Methods Mol. Biol. 769 (2011) 97–110.
[26] Y. Kidera, M. Tsubaki, Y. Yamazoe, K. Shoji, H. Nakamura, M. Ogaki, T. Satou, T. Itoh, M. Isozaki, J. Kaneko, Y. Tanimori, M. Yanae, S. Nishida, Reduction of lung metastasis, cell invasion, and adhesion in mouse melanoma by statin-induced blockade of the Rho/Rho-associated coiled-coil-containing protein kinase pathway, J. Exp. Clin. Cancer Res. 29 (2010) 127.
[27] C. Dan, A. Kelly, O. Bernard, A. Minden, Cytoskeletal changes regulated by the PAK4 serine/threonine kinase are mediated by LIM kinase 1 and cofilin, J. Biol. Chem. 276 (2001) 32115–32121.
[28] D.C. Edwards, L.C. Sanders, G.M. Bokoch, G.N. Gill, Activation of LIM-kinase by Pak1 couples Rac/Cdc42 GTPase signalling to actin cytoskeletal dynamics, Nat. Cell Biol. 1 (1999) 253–259.
[29] G.M. Morris, R. Huey, W. Lindstrom, M.F. Sanner, R.K. Belew, D.S. Goodsell, A.J. Olson, AutoDock4 and AutoDockTools4: automated docking with selective receptor flexibility, J. Comput. Chem. 30 (2009) 2785–2791.